Model Ziegler–Natta α-Olefin Polymerization Catalysts Derived from $[\{(\eta^5\text{-}C_5Me_4)SiMe_2(\eta^1\text{-}NCMe_3)\}(PMe_3)Sc(\mu_2\text{-}H)]_2$ and $[\{(\eta^5\text{-}C_5Me_4)SiMe_2(\eta^1\text{-}NCMe_3)\}Sc(\mu_2\text{-}CH_2CH_2CH_3)]_2$. Synthesis, Structures, and Kinetic and Equilibrium Investigations of the Catalytically Active Species in Solution

Pamela J. Shapiro,[1] W. Donald Cotter, William P. Schaefer, Jay A. Labinger, and John E. Bercaw*

Contribution No. 8894 from the Arnold and Mabel Beckman Laboratories of Chemical Synthesis, California Institute of Technology, Pasadena, California 91125

Received November 18, 1993®

Abstract: The scandium hydride complex $[(Cp^*SiNR)(PMe_3)Sc(\mu\text{-}H)]_2$, (**1**) ($(Cp^*SiNR) = \{(\eta^5\text{-}C_5Me_4)SiMe_2(\eta^1\text{-}NCMe_3)\}$) is prepared by hydrogenation of $(Cp^*SiNR)ScCH(SiMe_3)_2$ in the presence of trimethylphosphine. The hydride complex is a catalyst precursor for the polymerization of α-olefins, yielding atactic products of low molecular weight (M_n = 3000–7000). GC/MS analysis of volatile, oligomeric products revealed that all scandium centers are active during the polymerization. Selectivity for head-to-tail insertion is high (>99%) and for the tetramer, pentamer, and hexamer formed during propene polymerization, the maximum theoretical numbers of head-to-tail stereoisomers are observed by capillary GC. The stoichiometric reaction between **1** and 2 equiv of ethylene produces the unusual ethylene-bridged dimer $[(Cp^*SiNR)(PMe_3)Sc]_2(\mu,\eta^2,\eta^2\text{-}C_2H_4)$ (**2**) and an equivalent of ethane, whereas the same reaction with propene affords the phosphine-free, alkyl-bridged scandium dimer $[(Cp^*SiNR)Sc]_2(\mu\text{-}CH_2CH_2CH_3)_2$ (**3**). The absence of coordinating phosphine allows the latter complex to function as a more active olefin polymerization catalyst precursor. **1** reacts with styrene to form a unique double-insertion product arising from sequential 1,2- and 2,1-styrene insertion. The structure of the catalytic intermediate in solution was determined by low-temperature ^{13}C-NMR studies of the model complexes $(Cp^*SiNR)[P(^{13}CH_3)_3]ScCH_2CH(CH_3)CH_2CH_2CH_3$ and $(Cp^*SiNR)(PMe_3)Sc^{13}CH_2CH(^{13}CH_3)_2$. One phosphine-bound species is observed in equilibrium with only one phosphine-free species. The symmetry properties of the latter indicate that it is a monomeric, hence 12-electron, scandium alkyl complex. Semiquantitative treatment of equilibrium concentration data supports this conclusion.

The well-defined Ziegler–Natta olefin polymerization catalysts based on group 8,[2] early transition metal,[3] or lanthanide metal[4] compounds provide an unprecedented opportunity to investigate the mechanism(s) for this important process. The structural units of the latter two systems, $Cp'_2M\text{–}R$ ($Cp'_2 = (\eta^5\text{-}C_5Me_5)_2, \{(\eta^5\text{-}C_5Me_4)_2SiMe_2\}$; M = Sc, Y, La, Nd, Sm, Lu; R = H, alkyl) and $[Cp'_2M\text{–}CH_3^+][B(R)(C_6F_5)_3^-]$ catalysts ($Cp' = (\eta^5\text{-}C_5H_5), (\eta^5\text{-}C_5Me_5)$; M = Zr, Hf; R = C_6F_5, CH_3),[5] are closely analogous to the putative active catalyst in the homogeneous "Kaminsky" systems prepared from group 4 metallocene dichlorides and large excesses of methylalumoxane.[6] The remarkable stereospecificities displayed by variously modified group 4 metallocene/methylalumoxane catalysts are undoubtedly attributable to specific steric interactions controlling the carbon–carbon bond forming step in chain propagation, yet the structure of the transition state has not been established definitively for these complex catalyst systems.[7] Furthermore, an understanding of the factors which influence chain propagation and the various steps resulting in chain transfer (*e.g.* β-hydrogen elimination, β-alkyl elimination, σ-bond metathesis, chain transfer to aluminum) could point the way to catalysts that operate without chain transfer, *i.e.* as "living" Ziegler–Natta polymerization systems producing homo-block copolymers of various polyolefins.

The permethylscandocene system is particularly well suited to mechanistic studies, since all derivatives are monomeric and the reactions are constrained to occur in the equatorial plane of the $[Cp^*_2Sc]$ ($Cp^* = (\eta^5\text{-}C_5Me_5)$) wedge where all three frontier orbitals are located. We have previously reported on our investigations of the mechanism of ethylene insertion into $Cp^*_2\text{-}Sc\text{–}R$ bonds (R = H, alkyl, *etc.*) and β-H elimination for $Cp^*_2\text{-}Sc\text{–}CH_2CH_2R'$ (R' = H, alkyl, aryl).[3b] Model, single-component

® Abstract published in *Advance ACS Abstracts,* April 15, 1994.

(1) Present address: Department of Chemistry, University of Idaho, Moscow, Idaho 83843.

(2) Brookhart, M.; Volpe, A. F., Jr.; Lincoln, D. M.; Horváth, I. T.; Millar, J. M. *J. Am. Chem. Soc.* **1990**, *112*, 5634.

(3) (a) Jordan, R. F.; LaPointe, R. E.; Bradley, P. K.; Baenziger, N. *Organometallics* **1989**, *111*, 2728. (b) Burger, B. J.; Thompson, M. E.; Cotter, W. D.; Bercaw, J. E. *J. Am. Chem. Soc.* **1990**, *112*, 1566. (c) Shapiro, P. J.; Bunel, E. E.; Schaefer, W. P.; Bercaw, J. E. *Organometallics* **1990**, *9*, 867. (d) Piers, W. E.; Shapiro, P. J.; Bunel, E. E.; Bercaw, J. E. *Synlett* **1990**, 74. (e) Eshuis, J. J. W.; Tan, Y. Y.; Teuben, J. H.; Renkema, J. *J. Mol. Catal.* **1990**, *62*, 277. (f) Eshuis, J. J. W.; Tan, Y. Y.; Meetsma, A.; Teuben, J. H.; Renkema, J.; Evens, G. G. *Organometallics* **1992**, *11*, 362.

(4) (a) Watson, P. L. *J. Am. Chem. Soc.* **1982**, *104*, 337. (b) Jeske, G.; Lauke, H.; Mauermann, H.; Sweptson, P. N.; Schumann, H.; Marks, T. J. *J. Am. Chem. Soc.* **1985**, *107*, 8091.

(5) (a) Hlatky, G. G.; Turner, H. W.; Eckman, R. R. *J. Am. Chem. Soc.* **1989**, *111*, 2728. (b) Turner, H. W. European Patent Application 277004, 1988. (c) Chien, J. C. W.; Tsai, W.-M.; Rausch, M. D. *J. Am. Chem. Soc.* **1991**, *113*, 8570. (d) Yang, X.; Stern, C. L.; Marks, T. J. *J. Am. Chem. Soc.* **1991**, *113*, 3623.

(6) (a) Kaminsky, W.; Kulper, K.; Brintzinger, H. H.; Wild, F. R. W. P. *Angew. Chem.* **1985**, *97*, 507; *Angew. Chem., Int. Ed. Engl.* **1985**, *24*, 507. (b) Ewen, J. A.; Jones, R. L.; Razavi, A.; Ferrara, J. D. *J. Am. Chem. Soc.* **1988**, *110*, 6255. (c) Ewen, J. A. *J. Am. Chem. Soc.* **1984**, *106*, 6355. (d) Erker, G.; Nolte, R.; Tsay, Y.-H.; Krüger, C. *Angew. Chem., Int. Ed. Engl.* **1989**, *29*, 629. (e) Mallin, D. T.; Rausch, M. D.; Lin, Y.-G.; Dong, S.; Chien, J. C. W. *J. Am. Chem. Soc.* **1990**. (f) Resconi, L.; Waymouth, R. M. *J. Am. Chem. Soc.* **1990**, *112*, 4953.

(7) (a) Piers, W. E.; Bercaw, J. E. *J. Am. Chem. Soc.* **1990**, *112*, 9406. (b) Krauledat; Brintzinger, H. H. *Angew. Chem., Int. Ed. Engl.* **1990**, *29*, 1412. (c) Laverty, D.; Rooney, J. J. *J. Chem. Soc., Farady Trans.* **1973**, *79*, 869. (d) Brookhart, M.; Green, M. L. H. *J. Organomet. Chem.* **1983**, *250*, 395. (e) Brookhart, M.; Green, M. L. H.; Wong, L. *Prog. Inorg. Chem.* **1988**, *36*, 1. (f) Clawson, L.; Soto, J.; Buchwald, S. L.; Steigerwald, M. L.; Grubbs, R. H. *J. Am. Chem. Soc.* **1985**, *107*, 3377.

0002-7863/94/1516-4623$04.50/0

Table 1. ^{1}H NMR Data[a]

compd	assignment	δ, ppm (coupling, Hz)
$[C_5(CH_3)_4H]Si(CH_3)_2[N(H)C(CH_3)_3]$[b,c]	$C_5(CH_3)_4H$	2.0
		1.8
"H_2Cp*SiNR"	$C_5(CH_3)_4H$	2.7
	$(CH_3)_3C$	1.1
	$(CH_3)_2Si$	0.1
$[$(Cp*SrNR)ScCl$]_x$[b,c]	$C_5(CH_3)_4$	2.0
		1.9
	$(CH_3)_3C$	1.3
	$(CH_3)_2Si$	0.7
(Cp*SiNR)ScCH[Si$(CH_3)_3]_2$[c]	$CH[Si(CH_3)_3]_2$	0.14
	$CH[Si(CH_3)_3]_2$	0.57
	$C_5(CH_3)_4$	2.05
		1.91
	$(CH_3)_3C$	1.3
	$(CH_3)_2Si$	0.66
$[$(Cp*SiNR)(PMe_3)Sc(H)$]_2$ (**1**)	Sc*H*	4.45 (br)
	$C_5(CH_3)_4$	2.21
		2.06
	$(CH_3)_3C$	1.28
	$(CH_3)_2Si$	0.68
	$(CH_3)_3P$	0.89
$[$(Cp*SiNR)(PMe_3)Sc(H)$]_2$ (**1**)[d]	Sc*H*	4.15 (br)
	$C_5(CH_3)_4$	2.36
		2.16
		1.99
		1.90
	$(CH_3)_3C$	1.31
	$(CH_3)_2Si$	0.84
		0.74
	$(CH_3)_3P$	0.89 (J_{PH} = 4)
$[$(Cp*SiNR)(PMe_3)Sc(μ-$^{13}C_2H_4$)$]_2$ (**2**)	CH_2CH_2	–0.17
	$C_5(CH_3)_4$	2.33
		1.89
	$(CH_3)_3C$	1.24
	$(CH_3)_2Si$	0.79
	$(CH_3)_3P$	0.88
$[$(Cp*SiNR)(PMe_3)Sc(μ-$^{13}C_2H_4$)$]_2$ (**2**)[e]	CH_2CH_2	0.18 (br d)
		–0.54 (br d)
	$C_5(CH_3)_4$	2.46
		2.35
		1.89
		1.86
	$(CH_3)_3C$	1.3
	$(CH_3)_2Si$	0.98
		0.90
	$(CH_3)_3P$	0.88 (J_{PH} = 4)
$[$(Cp*SiNR)Sc(μ-$CH_2CH_2CH_3$)$]_2$ (**3**)[c]	Sc$CH_2CH_2CH_3$	–0.11 (J_{HH} = 8.6)
	Sc$CH_2CH_2CH_3$	obscured by $C(CH_3)_3$
	Sc$CH_2CH_2CH_3$	1.06 (J_{HH} = 6.6)
	$C_5(CH_3)_4$	2.17
		1.91
	$(CH_3)_3C$	1.25
	$(CH_3)_2Si$	0.72
(Cp*SiNR)(PMe_3)Sc($CH_2CH_2CH_3$)	Sc$CH_2CH_2CH_3$	–0.09 (m)
	Sc$CH_2CH_2CH_3$	1.67 (m)
	Sc$CH_2CH_2CH_3$	1.15 (≈t)
	$C_5(CH_3)_4$	2.10
		2.05
	$(CH_3)_3C$	1.4
	$(CH_3)_2Si$	0.66
	$(CH_3)_3P$	0.74 (br)
$[$(Cp*SiNR)Sc(μ-$CH_2CH_2CH_2CH_3$)$]_2$[c]	Sc$CH_2CH_2CH_2CH_3$	–0.11 (J_{HH} ≈ 9)
	Sc$CH_2CH_2CH_2CH_3$	obscured by $C(CH_3)_3$
	Sc$CH_2CH_2CH_2CH_3$	1.38 (m)
	Sc$CH_2CH_2CH_2CH_3$	0.96 (J_{HH} = 7.2)
	$C_5(CH_3)_4$	2.18
		1.92
	$(CH_3)_3C$	1.28
	$(CH_3)_2Si$	0.74
(Cp*SiNR)(PMe_3)ScR (**4**)[d,f,g]	Sc$CH_2CH(CH_3)CH_2CH_2CH_3$	a: –0.08 (m)
R = $CH_2CH(CH_3)CH_2CH_2CH_3$		b: 0.14 (m)
		–0.17 (m)
	$C_5(CH_3)_4$	a: 2.43
		1.90
		b: 2.33
		2.34
		1.85
		1.84
	$(CH_3)_3C$	1.47
	$(CH_3)_2Si$	a: 0.88
		b: 0.704
		0.698
	$(CH_3)_3P$	0.5 (J_{PH} = 4.4)

Table 1 (Continued)

compd	assignment	δ, ppm (coupling, Hz)
(Cp*SiNR)(PMe$_3$)ScR[c]	ScC*H*(C$_6$H$_5$)CH$_2$CH$_2$CH$_2$(C$_6$H$_5$)	not assigned
R = CH(C$_6$H$_5$)CH$_2$CH$_2$CH$_2$(C$_6$H$_5$)	ScCH(C$_6$H$_5$)C*H*$_2$CH$_2$C*H*$_2$(C$_6$H$_5$)	2.69 (m)
		2.02 (m)
	ScCH(C$_6$H$_5$)CH$_2$C*H*$_2$CH$_2$(C$_6$H$_5$)	1.85 (m)
		1.65 (m)
	2 C$_6$H$_5$	7.3 (t)
		7.0–7.2 (m)
		6.53 (d)
		5.59 (t)
	C$_5$(C*H*$_3$)$_4$	2.25
		2.10
		2.06
		1.93
	(C*H*$_3$)$_3$C	1.27
	(C*H*$_3$)$_2$Si	0.77
		0.64
P(^{13}CH$_3$)$_3$[h]	^{13}C*H*$_3$	0.79 ($^1J_{CH}$ = 126.9)
		($^3J_{CH}$ = 5.1)
		($^2J_{PH}$ = 2.8)
(Cp*SiNR)[P(^{13}CH$_3$)$_3$]ScR (4-^{13}C$_3$)[h]	C*H*$_2$CH(CH$_3$)CH$_2$CH$_2$CH$_3$	0.05–0.02 (br, m)
R = CH$_2$CH(CH$_3$)CH$_2$CH$_2$CH$_3$	CH$_2$CH(CH$_3$)CH$_2$CH$_2$C*H*$_3$	1.05 (J_{HH} = 7.5)
	C$_5$(C*H*$_3$)$_4$	2.36
		2.28
		1.95
		1.88
	(C*H*$_3$)$_3$C	1.42 (br)
	(C*H*$_3$)$_2$Si	0.80
		0.64
	(^{13}C*H*$_3$)$_3$P	0.67 ($^1J_{CH}$ = 129)
H$_2$^{13}C=C(^{13}CH$_3$)$_2$[h]	*H*$_2$^{13}C	4.70 ($^1J_{CH}$ = 154)
	^{13}C*H*$_3$	1.60 ($^1J_{CH}$ = 125)
(Cp*SiNR)(PMe$_3$)Sc^{13}CH$_2$CH(^{13}CH$_3$)$_2$[h]	Sc^{13}C*H*$_2$CH(^{13}CH$_3$)$_2$	–0.03 ($^1J_{CH}$ = 103)
	Sc^{13}CH$_2$CH(^{13}C*H*$_3$)$_2$	2.31 ($^1J_{CH}$ = 117)
	C$_5$(C*H*$_3$)$_4$	2.36
		2.28
		1.95
		1.87
	(C*H*$_3$)$_3$C	1.43
	(C*H*$_3$)$_2$Si	0.80
		0.69
	(C*H*$_3$)$_3$P	0.65 (br)

[a] Spectra were obtained in toluene-d_8 at ambient temperature, 400 MHz, unless otherwise stated. Chemical shifts are reported in parts per million (δ) from tetramethylsilane referenced from solvent signal. [b] 90 MHz. [c] Benzene-d_6. [d] –80 °C. [e] –90 °C. [f] 500 MHz. [g] Two diastereomers (denoted a and b) are observed. [h] 300 MHz.

systems readily polymerize ethylene, but few are capable of oligomerizing or polymerizing α-olefins, even propylene. In order to achieve sufficient reactivity to promote polymerization of α olefins, we progressed from the most crowded bis(pentamethylcyclopentadienyl) ligand system, to linked bis(alkyl-substituted cyclopentadienyl), and finally to the least crowded, linked amido–cyclopentadienyl ligand derivatives, [(Cp*SiNR)(PMe$_3$)Sc]$_2$(μ-H)$_2$ and [(Cp*SiNR)Sc]$_2$(μ-CH$_2$CH$_2$CH$_3$)$_2$ ((Cp*SiNR) = {(η^5-C$_5$Me$_4$)SiMe$_2$(η^1-NCMe$_3$)}).[3c,d,8,9] In so doing, we sacrificed some of the simplicity of the permethylscandocene system. Hydrides and alkyls of the type [(Cp*SiNR)Sc–R] (R = H, alkyl) readily dimerize and coordinate additional ligands (*e.g.* PMe$_3$). Hence, unlike for the bis(pentamethylcyclopentadienyl)scandium system, it appeared likely that the isolated, structurally characterized complexes are no longer the actual catalysts, but rather *pre*-catalysts for polymerization.

In order to determine the nature of the true catalytically active complex(es) (*i.e.* monomer *vs* dimer, phosphine-bound *vs* phosphine-free), we have undertaken an investigation of this [(Cp*SiNR)Sc–R] α-olefin polymerization system, including synthetic and structural studies of the precatalysts, analysis of oligomeric and polymeric products, and kinetic and equilibrium studies. The results of those experiments are described herein. All evidence points to a monomeric, Lewis base-free, 12-electron scandium alkyl as the active chain propagating species.

Scheme 1

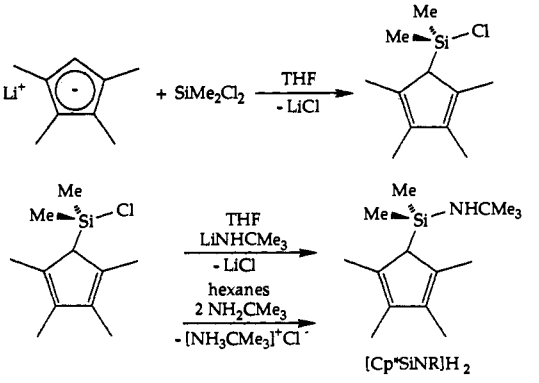

Results and Discussion

Synthesis and Characterization of [(Cp*SiNR)(PMe$_3$)Sc]$_2$(μ-H)$_2$ (1). The diprotonated, [SiMe$_2$]-linked tetramethylcyclopentadienide–*tert*-butylamido ligand, [Cp*SiNR]H$_2$, (Cp*SiNR = {(η^5-C$_5$Me$_4$)SiMe$_2$(η^1-NCMe$_3$)}) is prepared straightforwardly by treating SiMe$_2$Cl$_2$ first with Li(C$_5$Me$_4$H) and then with lithium *tert*-butyl amide (Scheme 1). It is convenient that the preferential reaction is between lithium *tert*-butylamide and the [Si–Cl] of (C$_5$Me$_4$H)SiMe$_2$Cl rather than deprotonation of the substituted cyclopentadiene. Alternatively, treatment of (C$_5$Me$_4$H)SiMe$_2$-

(8) There has been some recent interest in the application of this ligand system to Ti-, Zr-, and Hf-based catalysts for ethylene/1-alkene copolymerizations; see, for example: Canich, J. M. Eur. Patent 420 436, 1991; Canich, J. M.; Hlatky, G. G.; Turner, H. W. U.S. Patent 542 236, 1990; Stevens, J. C.; Timmers, F. J.; Wilson, D. R.; Schmidt, G. F.; Nickias, P. N.; Rosen, R. K.; Knight, G. W.; Lai, S. Eur. Patent 416 815, 1990.

(9) Very recently a related but unlinked ligand system has been employed with yttrium to achieve olefin polymerizations: Schaverien, C. J. *Organometallics* **1994**, *13*, 69.

Cl with 2 equiv of *tert*-butylamine cleanly affords [Cp*SiNR]-H_2. The latter procedure is somewhat more convenient, since the crude hexane filtrate from the first step may be used directly. Both procedures produce [Cp*SiNR]H_2 in yields around 80%.

Vacuum distillation of crude [Cp*SiNR]H_2 followed by double deprotonation with *n*-butyllithium yields pure samples of the dilithium salt (eq 1). An X-ray structure determination for $K(THF)(C_5Me_4)SiMe_2(NHCMe_3)$, prepared by treatment of [Cp*SiNR]H_2 with KH, has been reported elsewhere.[10] Reaction

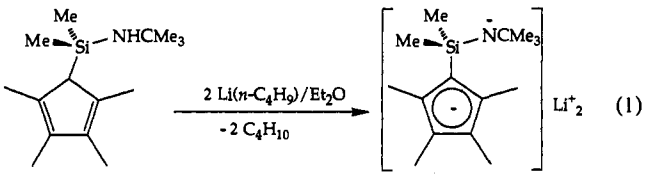

(1)

of the dilithium salt with $ScCl_3(THF)_3$ affords (Cp*SiNR)ScCl that is complexed by variable, nonstoichiometric amounts of THF and LiCl (eq 2). The presence of THF is undesirable since it

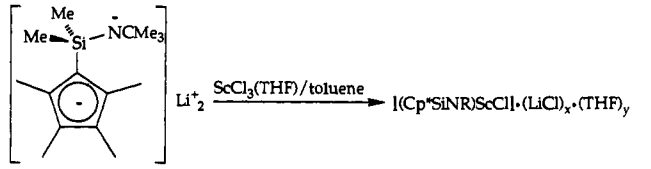

(2)

blocks the alkylation of the Sc–Cl bond. THF may be removed by heating the solid $[(Cp^*SiNR)ScCl]\cdot(LiCl)_x\cdot(THF)_y$ at 100 °C *in vacuo* for 1 day. Lithium chloride may be removed by Soxhlet extraction of $[(Cp^*SiNR)ScCl]_x$ from the residue with hot toluene, although complexed lithium chloride does not interfere with the subsequent alkylation step (*vide infra*).

The bulky bis(trimethylsilyl)methyl derivative, (Cp*SiNR)-Sc–$CH(SiMe_3)_2$, is the only alkyl derivative that has been successfully prepared thus far from $[(Cp^*SiNR)ScCl]_x$ (eq 3).

$$1/x\ [(Cp^*SiNR)ScCl]_x + LiCH(SiMe_3)_2 \rightarrow (Cp^*SiNR)Sc\text{–}CH(SiMe_3)_2 + LiCl \quad (3)$$

The reactions of other alkyllithium reagents such as $LiCH_3$, LiC_6H_5, and even $LiCH_2SiMe_3$ with the scandium chloride complex do not afford clean products. Despite several attempts, single crystals of (Cp*SiNR)Sc–$CH(SiMe_3)_2$ suitable for X-ray analysis could not be obtained and ebulliometric molecular weight analyses were inconclusive in determining its molecularity in solution, likely due to slow decomposition. It may be hydrogenated cleanly in the presence of PMe_3 to form the hydride complex $[(Cp^*SiNR)(PMe_3)Sc]_2(\mu\text{-}H)_2$ (**1**) in 83% isolated yield (eq 4).

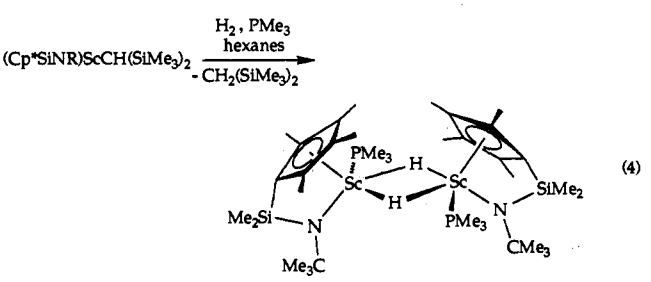

(4)

An X-ray structure determination reported earlier[11] revealed a double hydrogen-bridged dimer of C_2 symmetry for its solid-state structure; however, its poor solubility and extreme reactivity have prevented determination of its solution molecular weight by ebulliometric methods. A monomer/dimer equilibrium in solution is suggested by the presence of two peaks (neither of which corresponds to free PMe_3) in a *ca.* 4:1 ratio in the ^{31}P NMR spectrum of **1** measured at –66 °C in toluene-d_8; a single resonance is observed at 20 °C. A variable-temperature ^1H NMR study revealed only a single detectable species over the range –80 to 25 °C. Apparently, the two species undergoing equilibration on the ^{31}P NMR time scale are interconverting too rapidly for their interconversion to be "frozen out" on the ^1H NMR time scale.

The hydride resonance occurs at δ 4.45 in the ^1H NMR spectrum and is considerably broadened due to its proximity to the quadrupolar scandium nucleus ($I = {}^7/_2$, 100% abundance). A broad band of medium intensity at 1152 cm^{-1} is observed in the infrared spectrum for **1**. Although this frequency is extremely low for a metal hydride stretching mode, even for a (doubly) bridging one, the spectrum for $[(Cp^*SiNR)(PMe_3)Sc]_2(\mu\text{-}D)_2$, prepared by treatment of (Cp*SiNR)Sc–$CH(SiMe_3)_2$ with D_2 and PMe_3, is lacking this band. Unfortunately, there are interfering bands in the region of *ca.* 815 cm^{-1}, so that no new band attributable to a scandium–deuteride vibration was observed. Thus, we tentatively ascribe the 1152-cm^{-1} band to the asymmetric $\nu(Sc_2H_2)$ stretching mode.

Dissociation of the trimethylphosphine ligands for **1** is sufficiently rapid to average the ^1H NMR signals of the diastereotopic methyl substituents on the cyclopentadienyl ring and the silylene bridge of the (Cp*SiNR) ligand at room temperature (Scheme 2). To determine if a bis(phosphine) adduct, $(Cp^*SiNR)(PMe_3)_2$-ScH, analogous to $[Cp_2Zr(PMe_3)_2(H)][B(C_6H_5)_4]$[12] might be formed, a 10-fold excess of PMe_3 was added to a solution of **1**. Apart from that for free trimethylphosphine, no new resonances were detected (^1H or ^{31}P NMR, 25 to –80 °C).

$[(Cp^*SiNR)(PMe_3)Sc]_2(\mu_2,\eta^2,\eta^2\text{-}C_2H_4)$: An Unusual Ethylene Bridged Dimer from the Stoichiometric Reaction of $[(Cp^*SiNR)(PMe_3)Sc]_2(\mu\text{-}H)_2$ with Ethylene. The simplest olefin insertion reaction involves addition of ethylene to the Sc–H bond for $[(Cp^*SiNR)(PMe_3)ScH]$. Addition of 2 equiv of ethylene to $[(Cp^*SiNR)(PMe_3)Sc]_2(\mu\text{-}H)_2$ affords an unexpected product, however. Instead of the familiar triplet, quartet pattern of an ethyl group, a singlet at δ –0.17 is observed in the ^1H NMR spectrum. Moreover, when the reaction is performed with $^{13}C_2H_4$, the (proton coupled) ^{13}C NMR spectrum of the product exhibits a triplet pattern with $^1J_{CH}$ = 142 Hz. Fine structure due to second-order coupling effects is also apparent.

Closer inspection of the ^1H NMR spectra of the reaction mixture reveals a resonance consistent with free ethane located at δ 0.75, suggesting that the reaction product is, in fact, the ethylene-bridged scandium dimer $[(Cp^*SiNR)(PMe_3)Sc]_2(\mu_2,\eta^2,\eta^2\text{-}C_2H_4)$ (**2**, Scheme 3).

An X-ray crystal structure determination was undertaken to confirm this assignment (Figure 1). The arrangements of the (Cp*SiNR) and PMe_3 ligands for $[(Cp^*SiNR)(PMe_3)Sc]_2(\mu\text{-}H)_2$ and $[(Cp^*SiNR)(PMe_3)Sc]_2(\mu_2,\eta^2,\eta^2\text{-}C_2H_4)$ are nearly identical, although the Sc–P bond length (2.825(3) Å) is significantly shorter for the latter. The $Sc_2(\mu_2,\eta^2,\eta^2\text{-}C_2H_4)$ group is clearly the most unusual feature of the structure, having been observed in only a few other cases.[13] The C–C bond length of the ethylene bridge (1.433(12) Å) is intermediate between that of a single and a double C–C bond, comparable to the bond lengths observed in transition metal olefin complexes. The sp^2 hybridization of the μ-ethylene carbons is reflected in the H–C–H angle of 120(6)° as well as the large $^1J_{CH}$ of 142 Hz.

There are precedents for this type of ethylene-bridged structure in homogeneous Ziegler–Natta catalyst systems based on titanocene and zirconocene derivatives.[11a,b] The $M_2(\mu_2,\eta^2,\eta^2\text{-}C_2H_4)$

(10) Schaefer, W. P.; Cotter, W. D.; Bercaw, J. E. *Acta Crystallogr., Sect. C* **1993**, *49*, 1489.

(11) Shapiro, P. J.; Bunel, E. E.; Schaefer, W. P.; Bercaw, J. E. *Organometallics* **1990**, *9*, 867–869.

(12) Jordan, R. F.; Bajgur, C. S.; Dasher, W. E. *Organometallics* **1987**, *6*, 1041.

(13) (a) Kaminsky, W.; Sinn, H. *Liebigs Ann. Chem.* **1975**, 424, 438. (b) Kaminsky, W.; Kopf, J.; Sinn, H.; Vollmer, H. J. *Angew. Chem., Int. Ed. Engl.* **1976**, *15*, 629. (c) Wengrovius, J. H.; Schrock, R. R.; Day, C. S. *Inorg. Chem.* **1981**, *20*, 1844. (d) Cotton, F. A.; Kibula, P. A. *Polyhedron* **1987**, *6*, 645. (e) Cotton, F. A.; Kibula, P. A. *Inorg. Chem.* **1990**, *29*, 3192.

Table 2. ^{13}C NMR Data[a]

compd	assignment	δ, ppm (coupling, Hz)
[(Cp*SiNR)(PMe$_3$)Sc(H)]$_2$ (**1**)	$C_5(CH_3)_4$	15.0
		14.2
	$(CH_3)_3C$	36.9
	$(CH_3)_3C$	56.8
	$(CH_3)_2Si$	7.9
	$(CH_3)_3P$	16.2[b]
		13.0
[(Cp*SiNR)(PMe$_3$)Sc]$_2$(μ-$^{13}C_2H_4$) (**2**)	$^{13}CH_2{}^{13}CH_2$	35.2 (J_{CH} = 142)
[(Cp*SiNR)Sc(μ-$CH_2CH_2CH_3$)]$_2$ (**3**)	$ScCH_2CH_2CH_3$	50.5 (J_{CH} = 102)
	$ScCH_2CH_2CH_3$	20.8 (J_{CH} = 124)
	$ScCH_2CH_2CH_3$	21.2 (J_{CH} = 126)
	$C_5(CH_3)_4$	14.8 (J_{CH} = 125)
		12.6 (J_{CH} = 126)
	$C_5(CH_3)_4$	111.8
		110.7
	$(CH_3)_3C$	36.7 (J_{CH} = 125)
	$(CH_3)_3C$	55.2
	$(CH_3)_2Si$	8.0 (J_{CH} = 118)
[(Cp*SiNR)Sc(μ-$CH_2CH_2CH_2CH_3$)]$_2$	$ScCH_2CH_2CH_2CH_3$	46.7 (J_{CH} = 101)
	$ScCH_2CH_2CH_2CH_3$; $ScCH_2CH_2CH_2CH_3$	29.6 (J_{CH} = 122)
		30.5 (J_{CH} = 125)
	$ScCH_2CH_2CH_2CH_3$	14.0 (J_{CH} = 124)
	$C_5(CH_3)_4$	14.8 (J_{CH} = 125)
		12.5 (J_{CH} = 125)
	$C_5(CH_3)_4$	113.9
		111.6
	$(CH_3)_3C$	36.6 (J_{CH} = 124)
	$(CH_3)_3C$	55.2
	$(CH_3)_2Si$	8.0 (J_{CH} = 118)
(Cp*SiNR)(PMe$_3$)ScR[c]	$ScCH(C_6H_5)CH_2CH_2CH_2(C_6H_5)$	60.6 (J_{CH} = 120)
R = $CH(C_6H_5)CH_2CH_2CH_2(C_6H_5)$	$ScCH(C_6H_5)CH_2CH_2CH_2(C_6H_5)$	36.8 (J_{CH} = 125)
		33.5 (J_{CH} = 125)
		30.7 (J_{CH} = 120)
	2 C_6H_5[d]	151.5
		143.6
		117.8 (J_{CH} = 158)
		121.5 (J_{CH} = 158)
		125.7 (J_{CH} = 158)
		126.0 (J_{CH} = 158)
		130.3 (J_{CH} = 158)
P($^{13}CH_3$)$_3$	$^{13}CH_3$	16.39 (J_{PC} = 13.5)
(Cp*SiNR)[P($^{13}CH_3$)$_3$]ScR (4-$^{13}C_3$)[e-g]	$^{13}CH_3$ (free phosphine)	15.97 (br d)
R = $CH_2CH(CH_3)CH_2CH_2CH_3$	$^{13}CH_3$ (bound phosphine)	12.96 (J_{PC} = 12.6)
		12.92 (J_{PC} = 12.6)
$H_2{}^{13}C{=}C(^{13}CH_3)_2$[h]	$H_2{}^{13}C$	111.13 (J_{CC} = 3 Hz)
	$^{13}CH_3$	24.07 (J_{CC} = 3 Hz)
(Cp*SiNR)(PMe$_3$)Sc$^{13}CH_2CH(^{13}CH_3)_2$[h]	$Sc^{13}CH_2CH(^{13}CH_3)_2$	64. (br)
	$Sc^{13}CH_2CH(^{13}CH_3)_2$	28.5 (J_{CC} = 3 Hz)
		30.5 (J_{CC} = 3 Hz)
(Cp*SiNR)(PMe$_3$)Sc$^{13}CH_2CH(^{13}CH_3)_2$[e-g]	$Sc^{13}CH_2CH(^{13}CH_3)_2$	61.34
	$Sc^{13}CH_2CH(^{13}CH_3)_2$ (phosphine-bound species)	31.48[i]
		29.71
	$Sc^{13}CH_2CH(^{13}CH_3)_2$ (phosphine-free species)	24.74

[a] Spectra were taken in toluene-d_8 at ambient temperature, 100 MHz, unless otherwise stated. Chemical shifts are reported in parts per million (δ) from tetramethylsilane referenced from solvent signal. Coupling constants (J_{CH}) were obtained from a gated (^{1}H NOE enhanced) spectrum and are reportd in hertz. [b] Because of the limited solubility of this compound, some excess trimethylphosphine is apparently leached into solution from the undissolved compound, giving rise to the signal at 16.2 ppm. [c] Benzene-d_6. [d] Some peaks are obscured by solvent. [e] 125 MHz. [f] –73 °C. [g] 4 × 10^{-2} M. [h] 75 MHz. [i] $^3J_{CC}$ obscured by 10-Hz line broadening.

core for [(Cp*SiNR)(PMe$_3$)Sc]$_2$(μ_2,η^2,η^2-C_2H_4) is comparable to the most symmetric of those prepared to date with the two Sc–C bond lengths nearly the same (2.357(9) and 2.320(9) Å).

To elucidate the mechanism of formation of **2**, the reaction of **1** with ethylene was followed by low-temperature ^{1}H NMR spectroscopy. After the reagents were mixed in a precooled NMR tube and the reaction mixture was monitored as the temperature slowly warmed from –80 °C, it was noted that by *ca.* 0 °C all the ethylene (1 equiv per scandium) was consumed to form a new species, presumably an ethyl derivative. Due to the fluxionality of this intermediate, likely resulting from rapid dissociation of PMe$_3$, a clear spectrum was obtained only by cooling the sample to –90 °C. At this lower temperature a broad multiplet at *ca.* δ 0.0 corresponding to the α-methylene and a multiplet at *ca.* δ 0.96 for the β-methyl group are observed in addition to the signals for the Cp*SiNR ligand and coordinated PMe$_3$. On further warming to 25 °C, the intermediate converts to the ethylene bridged final product **2**. The production of 0.50 equiv of ethane per 1 equiv of ethylene consumed in this reaction was confirmed by a Toepler pump experiment, in which 95.5% of the theoretical amount of ethane was collected. Further addition of ethylene to **2** results in rapid formation of polyethylene, presumably via insertion into either scandium–carbon bond.

A variable temperature ^{1}H NMR study for **2** indicates fluxional behavior. As with the hydride dimer, PMe$_3$ dissociation is sufficiently rapid to average the ^{1}H NMR signals of the diastereotopic methyl substituents on the cyclopentadienyl ring and the silylene bridge of the (Cp*SiNR) ligand at room temperature. A slower process resulting in an averaging of the signals of the inequivalent methylene protons of the Sc$_2$(μ_2,η^2,η^2-CHH′–CHH′) group is also observed. Coalescence of the signals

Scheme 2

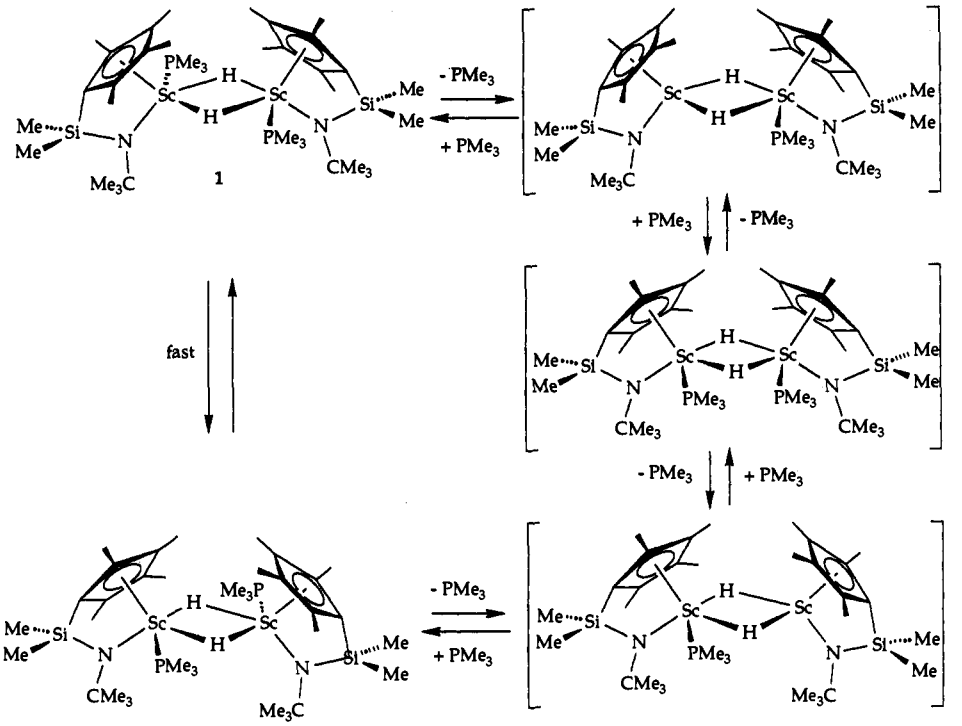

Table 3. ^{31}P NMR Data[a]

compd	assignment	δ, ppm (coupling, Hz)
[(Cp*SiNR)(PMe$_3$)Sc(H)]$_2$ (**1**)	(CH$_3$)$_3P^b$	−54.1
	(CH$_3$)$_3P^c$	−43.7
		−55.6
[(Cp*SiNR)(PMe$_3$)Sc(μ-^{13}C$_2$H$_4$)]$_2$ (**2**)	(CH$_3$)$_3P^d$	−42.2
	(CH$_3$)$_3P^e$	−39.4
(Cp*SiNR)(PMe$_3$)ScR R = CH$_2$CH(CH$_3$)CH$_2$CH$_2$CH$_3$	(CH$_3$)$_3P^c$	−51.5
(Cp*SiNR)(PMe$_3$)ScR R = CH(C$_6$H$_5$)CH$_2$CH$_2$CH$_2$(C$_6$H$_5$)	(CH$_3$)$_3P^e$	−45.9

[a] Spectra were taken in toluene-d_8 at the indicated temperatures, 36 MHz. Chemical shifts are reported in parts per million (δ) from H_3PO_4 referenced from an external standard. [b] 20 °C. [c] −66 °C. [d] 16 °C. [e] −50 °C.

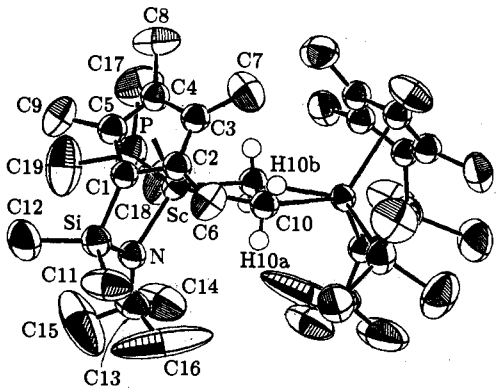

Figure 1. An ORTEP drawing of the dimer [(Cp*SiNR)(PMe$_3$)Sc]$_2$-(μ_2,η^2,η^2-C$_2$H$_4$) (**2**) shown at the 50% probability level, showing the numbering system. Hydrogen atoms are shown only on C10 (as spheres of arbitrary size).

for these protons occurs at 274 K, indicating an exchange rate constant of 1.6×10^3 s^{-1} and $\Delta G^{\ddagger} = 12$ kcal·mol^{-1} at this temperature. Significantly, this rate is unchanged on addition of *ca.* 3 equiv of trimethylphosphine.

The most likely mechanism for this interchange of hydrogens and carbons is given in Scheme 4. As shown, dissociation of two diagonally positioned Sc–C bonds of the Sc$_2$(μ_2,η^2,η^2-CH$_2$–CH$_2$) bridge affords a more conventional ethylene-bridged intermediate with free rotation about the Sc–C$_\alpha$ bonds. In order to effect the interconversion of H and H′ (and C$_\alpha$ and C$_{\alpha'}$), reversible

Table 4. Crystal Data for **2**

formula: $Sc_2Si_2P_2N_2C_{45}H_{84}$	formula weight: 861.22
crystal color: pale yellow	habit: hexagonal prisms
a = 23.706(5) Å	β = 111.57(1)°
b = 11.342(2) Å	z = 4
c = 21.141(3) Å	
v = 5286.2(7) Å^3	
λ = 0.71073 Å	T: 23 °C
graphite monochromator	absences: hkl, $h+k$ odd; $h0l$, l odd
space group: $C2/c$	μ = 4.03 cm^{-1} (μr_{max} = 0.13)
crystal size: ~0.35 × 0.4 × 0.4 mm	ω scan
CAD-4 diffractometer	octants collected: $\pm h, \pm k, -l$
	2θ range: 2–40°

no. of reflcns meas: 5205
no. of independent reflcns: 2475
no. with $F_o^2 > 0$: 2291
no. with $F_o^2 > 3\sigma(F_o^2)$: 1757
goodness of fit for merging data: 0.97
final R index: 0.086
final goodness of fit: 3.84

Scheme 3

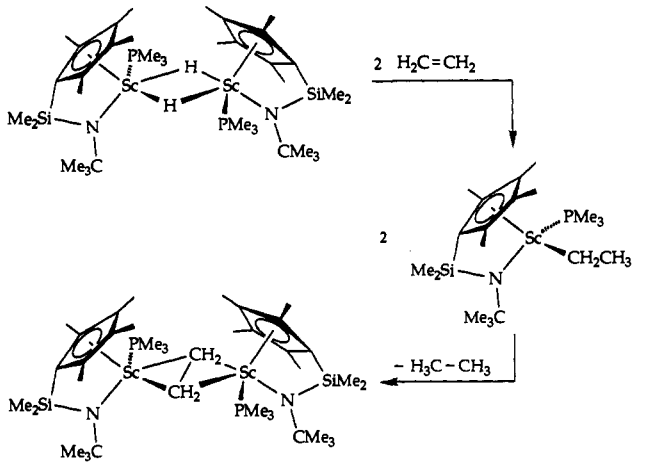

bridge affords a more conventional ethylene-bridged intermediate with free rotation about the Sc–C$_\alpha$ bonds. In order to effect the interconversion of H and H′ (and C$_\alpha$ and C$_{\alpha'}$), reversible

Table 5. Final Refined Parameters (x, y, z, and $U_{eq}{}^{a} \times 10^4$) for **2**

atom	x	y	z	U_{eq} or B
Sc	1008(1)	485(1)	2979(1)	452(4)
P	1128(1)	157(2)	4347(1)	729(8)
Si	2091(1)	−386(2)	2729(1)	653(7)
N	1478(2)	−988(5)	2863(3)	4.2(1)[b]
C1	1866(3)	1190(6)	2751(4)	4.1(2)[b]
C2	1361(3)	1717(6)	2237(4)	4.3(2)[b]
C3	1114(3)	2607(6)	2520(4)	4.4(2)[b]
C4	1449(3)	2635(7)	3213(4)	4.6(2)[b]
C5	1905(3)	1803(7)	3368(4)	4.7(2)[b]
C6	1132(4)	1412(7)	1489(4)	789(27)
C7	630(4)	3457(8)	2129(5)	953(30)
C8	1379(4)	3564(8)	3687(5)	977(30)
C9	2414(4)	1660(8)	4052(4)	894(30)
C10	28(4)	466(9)	2174(4)	4.3(2)[b]
C11	2174(5)	−766(8)	1914(5)	1142(34)
C12	2857(4)	−720(8)	3374(6)	1168(37)
C13	1349(4)	−2256(8)	2846(5)	744(29)
C14	848(5)	−2513(8)	3064(6)	1283(41)
C15	1854(6)	−2940(11)	3234(11)	2730(102)
C16	1129(10)	−2664(11)	2124(10)	3086(106)
C17	1019(5)	1443(10)	4784(5)	1218(38)
C18	553(4)	−767(9)	4465(4)	1044(33)
C19	1810(4)	−482(11)	4955(5)	1424(43)
H10A	−7(28)	1130(58)	3045(32)	6.2(20)[b]
H10B	−91(23)	−234(49)	3016(27)	3.8(15)[b]

[a] $U_{eq} = {}^1/_3\sum_i\sum_j[U_{ij}(a_i{}^*a_j{}^*)(\vec{a}_i\cdot\vec{a}_j)]$. [b] Isotropic displacement parameter, B.

Table 6. Selected Distances and Angles for **2**

	Distance (Å)		
Sc–P	2.825(3)	Si–C11	1.855(11)
Sc–N	2.071(6)	Si–C12	1.865(10)
Sc–C10	2.320(9)	N–C13	1.469(11)
Sc–C10′	2.357(9)	C13–C14	1.453(15)
C10–C10′	1.433(12)	C13–C15	1.41(2)
C10–H10A	0.88(7)	C13–C16	1.49(2)
C10–H10B	0.93(6)	P–C17	1.796(11)
Si–N	1.722(6)	P–C18	1.808(10)
Si–C1	1.871(8)	P–C19	1.807(11)
	Angle (deg)		
Sc–C10–C10′	73.6(5)	Sc–N–Si	102.9(3)
C10–Sc–C10′	35.7(3)	Sc–N–C13	132.6(5)

dissociation of both lateral (*anti* to PMe_3) and central (*syn* to PMe_3) scandium–carbon bonds must take place. This process thus involves a dyotropic rearrangement at the two carbons of the ethylene bridge, but with the unusual feature that the symmetric, 5-coordinate carbon[14] geometry is the ground-state arrangement, not the transition-state. Other mechanisms for the interconversion of H and H′, *i.e.* an in-place 180° rotation of the C_2H_4 unit about the Sc–Sc vector or reversible β-H elimination to [(Cp*SiNR)(PMe$_3$)ScH] and [(Cp*SiNR)(PMe$_3$)ScCH=CH$_2$], cannot be excluded; however, we favor the process shown in Scheme 4.

Isolation and Structural Characterization of Scandium Alkyl Dimers, [(Cp*SiNR)Sc]$_2$(μ-alkyl)$_2$. Reaction of **1** with 1 equiv of propylene per scandium yields the PMe_3-free scandium propyl derivative [(Cp*SiNR)Sc]$_2$(μ-CH$_2$CH$_2$CH$_3$)$_2$ (**3**, Scheme 5). An X-ray structure determination revealed it to be a dimer in the solid state with a double, three-center, two-electron propyl-bridged core, [Sc$_2$(μ-CH$_2$CH$_2$CH$_3$)$_2$]. As can be seen from the ORTEP drawing of **3** (Figure 2), and in contrast to approximately C_2-symmetric **1** and **2**, the two halves of **3** are related by a center of inversion. The Sc–C–Sc bridge angle of 89.4(2)° is considerably more acute than the corresponding Sc–H–Sc bridge angle in [(Cp*SiNR)(PMe$_3$)Sc]$_2$(μ-H)$_2$ (114.1°), reflecting the higher directionality of the carbon sp^3 orbital as compared with the s orbital of the μ-H, such that a narrowing of the bridge angle is necessary to achieve sufficient orbital overlap for the μ-alkyl. Similar structural trends are evident in other μ-H and μ-alkyl systems. For example, the 114(3)° Y–H–Y′ bridge angle in [(η^5-CH$_3$C$_5$H$_4$)$_2$Y(THF)]$_2$(μ-H)$_2$[15] contracts to 87.7(3)° in [(η^5-C$_5$H$_5$)$_2$Y]$_2$(μ-CH$_3$)$_2$,[16] angles surprisingly similar to those found in the scandium systems described here, considering yttrium's larger size. Likewise, the μ-H bridge angle of 103(2)° in the dimethylaluminum hydride dimer[17] is considerably larger than the 74.7(4)° μ-CH$_3$ bridge angle for the trimethylaluminum dimer.[18] As expected, the atoms connected to the amide nitrogen in **3** are coplanar to within ±0.01 Å, and the Si–N bond distance (1.720(5) Å) is similar to those for **1** and **2**. The bite angle of the chelating Cp*SiNR ligand (102.5°) is slightly smaller than that for the hydride dimer **1**, and the Sc–N bond distance (2.083(5) Å) is even longer than that in the ethylene-bridged complex **2**.

^{1}H and ^{13}C NMR data for toluene solutions of [(Cp*SiNR)Sc]$_2$(μ-CH$_2$CH$_2$CH$_3$)$_2$ are consistent with its solid-state structure. The ^{1}H NMR spectrum (toluene-d_8) is invariant over the temperature range 25 to −80 °C and displays a broad pseudotriplet ($^3J_{HH}$ = 8.6 Hz) upfield at δ −0.11 for Sc$_2$(CH$_2$CH$_2$CH$_3$)$_2$ along with a triplet at δ 1.06 ($^3J_{CH}$ = 6.6 Hz) for Sc$_2$(CH$_2$CH$_2$CH$_3$)$_2$. The β-methylene protons give rise to a complex pattern which is partly obscured by the *tert*-butyl resonance for the [NCMe$_3$] group. This complexity may be attributed to their diastereotopic nature as well as their coupling to both the α-methylene and γ-methyl hydrogens of the propyl group.

Upon addition of 1 equiv of PMe_3 an entirely new set of resonances is observed, probably as a result of formation of (Cp*SiNR)(PMe$_3$)ScCH$_2$CH$_2$CH$_3$. Site exchange of the PMe_3 in the propyl derivative is rapid, so that at −80 °C the methyl resonances of the (Cp*SiNR) ligand are broadened but not resolved into their diastereotopic components. Interestingly, excess PMe_3 appears to enhance the rate of PMe_3 site exchange, such that the ligand resonances are sharp (*i.e.* in the fast exchange limit) even at −80 °C in the presence of 5 equiv of PMe_3. Associative exchange, possibly via the bis(trimethylphosphine) adduct, (Cp*SiNR)(PMe$_3$)$_2$ScCH$_2$CH$_2$CH$_3$, readily accounts for this behavior (Scheme 6).

As is common to scandium alkyl complexes, the ^{13}C NMR resonance for the α-carbon for **3** is broad and shifted considerably downfield (δ 50.52). This signal appears as a triplet in the proton-coupled spectrum. The five-coordinate bridging geometry of the α-carbon is reflected in the low $^1J_{CH}$ of 103 Hz: *cf.* $^1J_{CH}$ of *ca.* 118–125 Hz for nonbridging Sc–alkyl systems.[19] Neither the crystal structure nor infrared spectral data suggest agostic C–H interactions for the propyl dimer **3**.

A similar PMe_3-free scandium *n*-butyl derivative is obtained when [(Cp*SiNR)(PMe$_3$)Sc]$_2$(μ-H)$_2$ is treated with 1-butene. The ^{1}H NMR spectrum for this product is essentially identical to that for **3**, with the exception of an extra multiplet at δ 1.38 for the γ-methylene hydrogens. Thus, a doubly-alkyl-bridged dimer is presumed to be formed in this case as well. Unfortunately, the low solubilities of both complexes and their reactivities toward benzene have prevented determination of their solution molecular weights.

Reaction of [(Cp*SiNR)(PMe$_3$)Sc]$_2$(μ-H)$_2$ with Other Olefins. While dimerization serves as a driving force for PMe_3 loss for the *n*-alkyl derivatives of [(Cp*SiNR)Sc], bulkier alkyl ligands such as 2-methylpentyl and isobutyl (*vide infra*) do not form stable

(14) For other examples of compounds with this type of bridging, 5-coordinate carbon center see: (a) Holton, J.; Lappert, M. F.; Pearce, R.; Yarrow, P. I. *Chem. Rev.* **1983**, *83*, 135. (b) Watson, P. L.; Parshall, G. W. *Acc. Chem. Res.* **1985**, *18*, 51. (c) Waymouth, R. M.; Santarsiero, B. D.; Coots, R. J.; Bronikowski, M. J.; Grubbs, R. H. *J. Am. Chem. Soc.* **1986**, *108*, 1427.

(15) Evans, W. J.; Meadows, J. H.; Wayda, A. L.; Hunter, W. E.; Atwood, J. L. *J. Am. Chem. Soc.* **1982**, *104*, 2008.

(16) Holton, J.; Lappert, M. F.; Ballard, D. G. H.; Pearce, R.; Atwood, J. L.; Hunter, W. E. *J. Chem. Soc., Dalton Trans.* **1979**, 54.

(17) Anderson, G. A.; Almenningen, A.; Forgaard, F. R.; Haaland, A. *J. Chem. Soc., Chem. Commun.* **1971**, 480.

(18) Huffman, J. C.; Streib, W. E. *J. Chem. Soc., Chem. Commun.* **1971**, 911.

(19) Burger, B. J. Ph.D. Thesis, California Institute of Technology, 1987.

Scheme 4

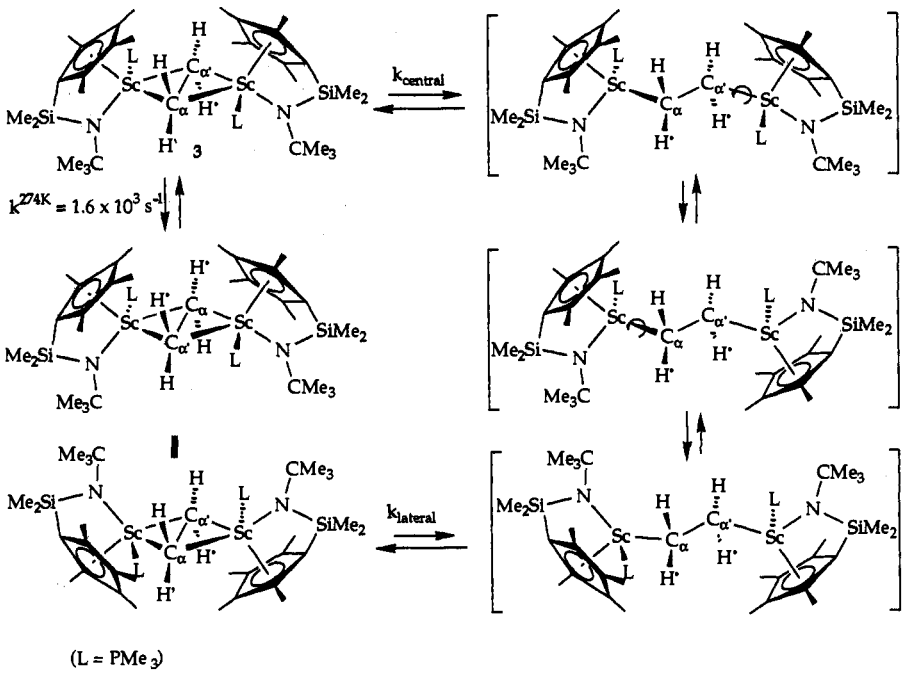

Scheme 5

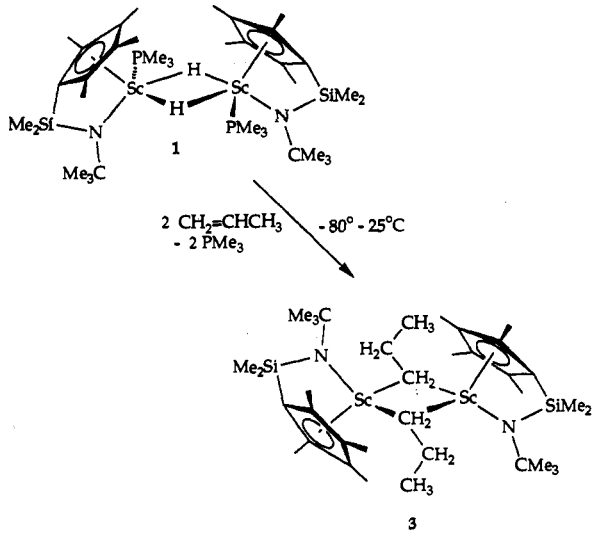

μ-alkyl bridges as readily and, therefore, more competitively retain PMe_3 in their coordination sphere. Hence, $(Cp^*SiNR)(PMe_3)$-$ScCH_2CH(CH_3)CH_2CH_2CH_3$ (**4**) is prepared by treating $[(Cp^*SiNR)(PMe_3)Sc]_2(\mu\text{-}H)_2$ with an excess of 2-methyl-1-pentene (Scheme 7).

Although the crude reaction mixture yields only a gold-brown oil upon removal of solvent and excess 2-methyl-1-pentene, cooling a concentrated solution of the compound in pentane affords white microcrystalline material in moderate yield (50%). Due to fluxionality, presumably involving phosphine site exchange, the room temperature ^1H NMR spectrum for $(Cp^*SiNR)(PMe_3)$-$ScCH_2CH(CH_3)CH_2CH_2CH_3$ is quite broad and uninterpretable. Upon cooling the sample to −80 °C, the spectrum reveals the presence of two species in roughly equal amounts, likely the two possible diastereomers. ^{13}C NMR spectroscopy also reveals the presence of two (presumably diastereomeric) products at low temperature. Once again, however, a reliable molecular weight measurement could not be obtained due to the instability of this reactive alkyl compound. Its formulation as (Cp^*SiNR)-$(PMe_3)ScCH_2CH(CH_3)CH_2CH_2CH_3$ is also confirmed by elemental analysis and by the observation that treatment with H_2 affords $[(Cp^*SiNR)(PMe_3)Sc]_2(\mu\text{-}H)_2$ together with 1.1 equiv of 2-methylpentane per scandium. As in the case of the hydride dimer **1**, we have seen no evidence for the formation of a bis(phosphine) adduct for **4**. Thus only resonances attributable to

Table 7. Crystal Data for **3**

formula: $(ScSiNC_{18}H_{34})_2$	formula wt: 337.52
a = 9.429(2) Å	space group: $P2_1/n$ (No. 14)
b = 21.937(5) Å	T = 21 °C
c = 9.826(2) Å	λ = 0.71073 Å
β = 99.39(2)°	ρ_{calc} = 1.12 g·cm^{-3}
Z = 2	$R(F_o)$ = 0.0854
V = 2005.2(7) Å^3	GOF = 2.36
crystal color: pale yellow	crystal habit: irregular plates
CAD-4	2θ range: 3–40°
ω scan	octants collected: $\pm h,\pm k,l$
graphite monochromator: yes	μ = 4.28 cm^{-1} (μr_{max} = 0.16)
crystal size: 0.2 × 0.2 × 0.8 mm	

total no. reflcns: 4082
total independent reflcns: 1863
GOF for merging: 0.977
R merge for reflections with exactly 2 observations: 0.041
no. of reflcns used in refinement: 1863
no. of reflcns with $F_o^2 > 0$ used in R: 1706
no. of reflcns with $F_o^2 > 3\sigma(F_o^2)$: 1231
R for reflections with $F_o^2 > 3\sigma(F_o^2)$: 0.0579

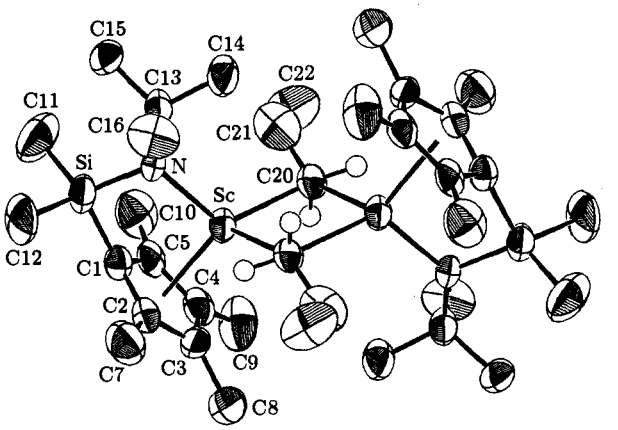

Figure 2. An ORTEP drawing of the dimer $[(Cp^*SiNR)Sc]_2(\mu\text{-}CH_2CH_2CH_3)_2$ (**3**) shown at the 50% probability level, showing the numbering system. Hydrogen atoms are shown only on C20 (as spheres of arbitrary size).

Table 8. Final Refined Parameters (x, y, z, and $U_{eq}{}^a \times 10^4$) for **3**

atom	x	y	z	U_{eq}
Sc	−85(2)	748(1)	5192(1)	460(4)
C1	464(8)	1783(3)	5817(8)	463(21)
C2	1742(9)	1557(3)	5417(8)	503(24)
C3	2422(8)	1151(3)	6419(9)	522(25)
C4	1560(10)	1115(3)	7452(8)	558(26)
C5	368(8)	1499(3)	7083(9)	521(25)
C7	2394(8)	1745(3)	4169(9)	868(27)
C8	3929(9)	912(3)	6481(10)	987(32)
C9	1952(9)	799(4)	8863(8)	974(31)
C10	−747(9)	1620(4)	7995(9)	878(27)
Si	−1108(2)	2023(1)	4535(2)	597(7)
C11	−2527(8)	2423(4)	5348(9)	1079(31)
C12	−609(9)	2594(3)	3292(10)	1046(32)
N	−1537(5)	1300(2)	3923(5)	419(16)
C13	−2684(8)	1166(3)	2711(8)	556(26)
C14	−3253(10)	537(4)	2865(10)	739(33)
C15	−3939(9)	1615(4)	2611(10)	698(31)
C16	−1995(11)	1205(5)	1386(10)	813(41)
C20	885(8)	111(3)	3677(8)	591(23)
C21	2222(10)	−173(4)	3397(9)	920(31)
C22	2646(9)	−64(4)	1971(9)	1080(33)

^{a} $U_{eq} = {}^1/_3\Sigma_i\Sigma_j[U_{ij}(a_i{}^*a_j{}^*)(\bar{a}_i\bar{a}_j)]$.

Table 9. Selected Distances and Angles for **3**

	Distance (Å)		
Sc–N	2.083(5)	Si–C1	1.858(7)
Sc–C20	2.334(7)	Si–C11	1.885(8)
Sc–C20′	2.372(7)	Si–C12	1.862(8)
Sc–Sc	3.310(2)	C20–C21	1.472(11)
C20–C20′	3.346(10)	C21–C22	1.538(12)
Sc–Cp*	2.210	N–C13	1.501(9)
Si–N	1.720(5)		
	Angle (deg)		
Sc–C20–C21	144.0(5)	Cp*–Sc–C20	119.6
Sc–C20–Sc′	89.4(2)	Cp*–Sc–C20′	118.5
Sc–C20′–C21	95.7(5)	Cp*–C1–Si	155.6
N–Sc–Cp*	102.5	Sc–Cp*–C1	82.8
C20–Sc–C20′	90.6(2)	N–Si–C1	95.3(3)
C22–C21–C20	117.5(7)		

free trimethylphosphine and **4** are observed in the slow-exchange, limiting (−80 °C) ^{1}H NMR spectrum of **4** in the presence of an additional equivalent of trimethylphosphine.

One reason for our interest in this derivative arose from the question of whether branching can occur in α-olefin polymerization by reinsertion of the olefinic polymer chain ends (formed in chain transfer by β-H elimination) into the propagating metal alkyl (*vide infra*). Since (Cp*SiNR)(PMe$_3$)ScCH$_2$CH(CH$_3$)CH$_2$CH$_2$CH$_3$ does not react further with 2-methyl-1-pentene, the formation of polyolefin with long branches arising from this process is unlikely. As expected, however, it does readily polymerize propylene.

Reaction of [(Cp*SiNR)(PMe$_3$)Sc]$_2$(μ-H)$_2$ with styrene proceeds in a rather different fashion. ^{1}H NMR integration and elemental analysis reveal that *two* molecules of styrene have reacted, and molecular weight measurements of the bright orange complex indicate a monomeric structure. ^{1}H-coupled ^{13}C NMR spectra suggest the connectivity as (Cp*SiNR)(PMe$_3$)ScCH(C$_6$H$_5$)CH$_2$CH$_2$CH$_2$C$_6$H$_5$, and ^{2}H NMR spectra are likewise consistent: reaction of [(Cp*SiNR)Sc]$_2$(μ-D)$_2$ with 2 equiv of CH$_2$=CHC$_6$H$_5$ affords (Cp*SiNR)(PMe$_3$)ScCH(C$_6$H$_5$)CH$_2$CH$_2$CHDC$_6$H$_5$ (δ 2.4); reaction of D$_2$ with (Cp*SiNR)(PMe$_3$)ScCH(C$_6$H$_5$)CH$_2$CH$_2$CH$_2$C$_6$H$_5$ affords CHD(C$_6$H$_5$)CH$_2$CH$_2$CH$_2$C$_6$H$_5$ (δ 2.4). Thus, as shown in Scheme 8, addition of styrene proceeds via a normal 1,2 (primary) insertion into the [Sc–H], followed by a rapid and terminal second insertion in the opposite, 2,1 manner for the phenethyl intermediate [(Cp*SiNR)ScCH$_2$CH$_2$C$_6$H$_5$].

The unusual preferences for styrene *vis-à-vis* other α olefins has also been observed in hydrozirconation.[20] It is likely that the reluctance of (Cp*SiNR)(PMe$_3$)ScCH(C$_6$H$_5$)CH$_2$CH$_2$CH$_2$C$_6$H$_5$ to undergo a third insertion of styrene is due to unfavorable steric interactions of the disubstituted α-carbon with another incoming styrene.

General Features of α-Olefin Polymerization by [(Cp*SiNR)(PMe$_3$)Sc]$_2$(μ-H)$_2$ and [(Cp*SiNR)Sc]$_2$(μ-CH$_2$CH$_2$CH$_3$)$_2$. Our initial discovery that the [(Cp*SiNR)Sc] system is capable of polymerizing α-olefins was with [(Cp*SiNR)(PMe$_3$)Sc]$_2$(μ-H)$_2$ (**1**) as catalyst (or catalyst precursor).[9] Internal olefins react with **1**, yielding a mixture of unidentified products but no polymers. The primary features of the polymerization using this precatalyst are summarized in Scheme 9.

Turnover rates for polymerizations are rather low; only gram quantities of polymer are isolated after several hours in neat olefin using *ca.* 50 mg of catalyst. Molecular weights for polymerizations carried out at 25 °C are indicative of oligomers rather than polymers (polypentene: $M_n \approx 3000$, PDI = 2.1; polybutene: $M_n \approx 4000$, PDI = 1.7). A modest increase to $M_n \approx 7000$ and a slight reduction in the polydispersity index to 1.7 is achieved by polymerizing 1-pentene at 0 °C. These low activities and the rather low solubilities of propylene at 25 °C and moderate pressures make the polymerization of propylene sluggish and impractical. The poly-1-butene and poly-1-pentene samples are colorless, sticky oils. Resonances for vinylidene chain ends are observed in their ^{1}H NMR spectra, implicating β-H elimination as a principal chain transfer pathway. As noted in the previous section, *gem*-disubstituted olefins (*e.g.* 2-methyl-1-pentene) react only slowly (overnight) with [(Cp*SiNR)(PMe$_3$)Sc]$_2$(μ-H)$_2$, and only in a stoichiometric fashion, indicating that chain transfer by β-H elimination in this catalyst system is only slowly reversed. Thus, reinsertion of the *gem*-disubstituted chain end does not compete effectively with the much faster addition of α-olefin. Moreover, branching of the polymer caused by the insertion of vinylidene chain ends into a growing [Sc–CH$_2$CHRCH$_2$CHRP] chain (**P** = polymer) does not occur.

Chain transfer by β-alkyl elimination would lead to vinylic chain ends.[21] Whereas signals due to CH$_2$=CHP are not apparent in the ^{1}H NMR spectra of polymers produced at room temperature, their absence does not necessarily rule out β-alkyl elimination. If these chain ends compete effectively with monomer for the [Sc–CH$_2$CHRCH$_2$CHRP] chain, they could be incorporated to produce long branches in the resultant polymer.[21,22] β-Methyl elimination, although slower than β-H elimination, is facile for the closely related system, {(η^5-C$_5$Me$_4$)$_2$SiMe$_2$}Sc–CH$_2$CHMe$_2$.[23]

There are two primary complications that could arise in undertaking a mechanistic study of a catalyst system such as [(Cp*SiNR)(PMe$_3$)Sc]$_2$(μ-H)$_2$: (*i*) only a minor component of the mixture is responsible for the catalysis, and (*ii*) more than one active species is present. Several observations indicate that these complications do not arise in the present case. Participation of all scandium centers in the polymerization is indicated by the disappearance of ^{1}H NMR signals characteristic of [(Cp*SiNR)(PMe$_3$)Sc]$_2$(μ-H)$_2$ upon addition of α-olefin; these resonances are regenerated when the reaction mixture is subsequently treated with H$_2$. The polydispersities of the polymers produced, as determined by gpc *vs* polystyrene, are approximately 2.[24]

(20) Nelson, J. E.; Bercaw, J. E.; Labinger, J. A. *Organometallics* **1989**, *8*, 2484.

(21) (a) Bunel, E. E.; Burger, B. J.; Bercaw, J. E. *J. Am. Chem. Soc.* **1988**, *110*, 976. (b) Piers, W. E.; Shapiro, P. J.; Bunel, E. E.; Bercaw, J. E. *Synlett* **1990**, 74. (c) Eshuis, J. J. W.; Tan, Y. Y.; Meetsma, A.; Teuben, J. H.; Renkema, J.; Evens , G. G. *Organometallics* **1992**, *11*, 362. (d) Resconi, L.; Piemontesi, F.; Franciscono, G.; Abis, L.; Fiorani, T. *J. Am. Chem. Soc.* **1992**, *114*, 1025.

(22) When polypropene is prepared at 80 °C with [(Cp*SiNR)(PMe$_3$)Sc]$_2$(μ-H)$_2$, a pattern that is diagnostic of vinylic chain ends is indeed observed in the olefinic region of the ^{1}H-NMR spectrum. Thus, β-alkyl elimination is evident, at least at elevated temperatures. On the other hand, the scandium catalyst is not stable at this temperature, forming a new, as yet unidentified species that crystallizes from the solution as it cools. ^{1}H- and ^{13}C-NMR spectra suggest that metallation of the C–H bonds of PMe$_3$ accompanies the thermal decomposition.

(23) Hajela, S.; Bercaw, J. E. *Organometallics*, in press.

Scheme 6

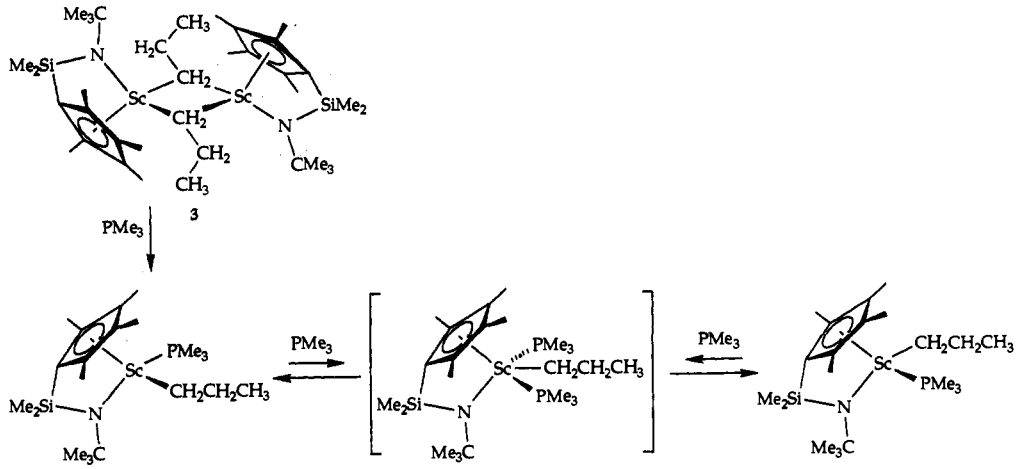

Scheme 7

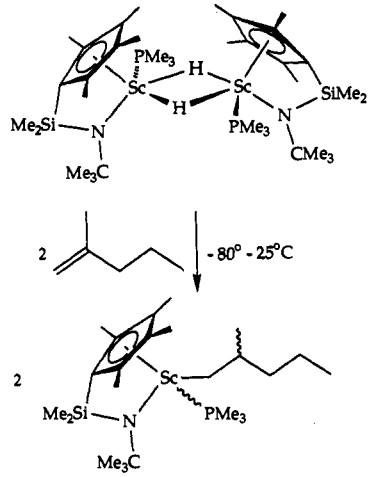

Scheme 8

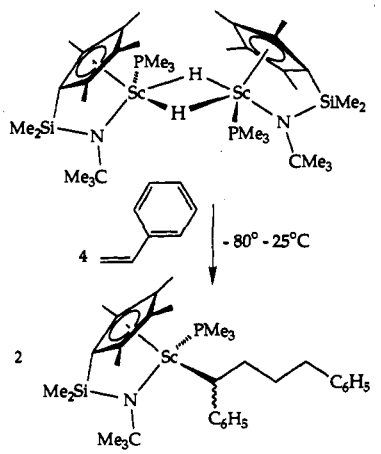

The molecular weight distributions for propylene oligomers produced by $[(Cp^*SiNR)(PMe_3)Sc]_2(\mu\text{-}H)_2$ were examined at low monomer conversion where chain transfer by β-H elimination has not occurred to a significant extent. If the rate of initiation is at least as fast as the rate of subsequent insertions and all of the scandium centers are active and inserting monomer at a uniform rate, the molecular weight distribution of oligomers produced should be modeled by a Poisson function based on the ratio of monomer consumed to scandium present. The molecular weight distributions of the saturated oligomers were analyzed by GC and GC/MS. As shown in Figure 3 for two representative oligomer distributions, the experimental data fit well with the calculated Poisson distributions on the basis of the amount of monomer consumed, *assuming all scandium centers are active*. As discussed previously,[25] this test is particularly sensitive to the fraction of scandium centers participating as well as to the criterion that chain propagation is occurring no more rapidly than chain initiation.

The maximum theoretical number of head-to-tail stereoisomers are observed by capillary GC for the shorter propylene oligomers: two for the tetramer, 2,4,6-trimethylnonane; four for the pentamer, 2,4,6,8-tetramethylundecane; and eight for the hexamer, 2,4,6,8,10-pentamethyltridecane. This observation of roughly equal amounts of each stereoisomer, as well as the physical characteristics of the polymers produced by $[(Cp^*SiNR)(PMe_3)Sc]_2(\mu\text{-}H)_2$, suggests that essentially atactic polymers are produced by this catalyst system.

Addition of trimethylphosphine to solutions of **1** slows the rate of α-olefin polymerization, suggesting that a PMe_3-free scandium alkyl is the true catalyst in this system (*vide infra*). Thus, it was not surprising to find that the dimeric alkyl complexes, $[(Cp^*SiNR)Sc]_2(\mu\text{-}CH_2CH_2CH_3)_2$ (**3**) and $[(Cp^*SiNR)Sc]_2(\mu\text{-}CH_2CH_2CH_2CH_3)_2$, are considerably more active catalyst precursors, and that the polymers produced have higher molecular weights (eq 5). Molecular weights for polymerizations carried

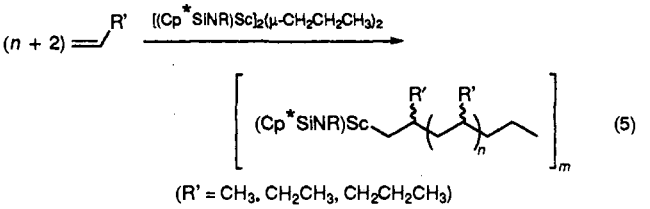

(5)

out using **3** as catalyst at 25 °C are $M_n \approx 6000$, PDI = 1.5 for poly(1-pentene) and $M_n \approx 9600$, PDI = 1.8 for polypropylene (25 v/v % in toluene). Again, a modest increase in molecular weight ($M_n \approx 16500$, PDI = 1.7 (25 v/v % in toluene)) is achieved by polymerizing propylene at 0 °C. The oily, tacky nature of the polymer indicated that it was atactic. The atacticity of the polymer stereochemistry was confirmed upon ^{13}C NMR characterization.[26]

When the polymerization is monitored by ^1H NMR spectrometry, a considerable amount of the starting complex is observed to be unreacted, even after the consumption of several equivalents of olefin relative to scandium, suggesting that initiation with **3** is slow relative to propagation. To confirm that the ^1H NMR resonances were due to unreacted **3** and not simply a generic

(24) Admittedly, for polymers of such low molecular weights, the PDI criterion is not particularly strong.

(25) Burger, B. J.; Thompson, M. E.; Cotter, W. D.; Bercaw, J. E. *J. Am. Chem. Soc.* **1990**, *112*, 1566.

(26) Interestingly, in the ^{13}C-NMR spectrum, the peaks for mm diads are of much lower than statistical intensity. Nevertheless, peaks for all nine resolvable pentads are visible with the mr diads predominating.

Scheme 9

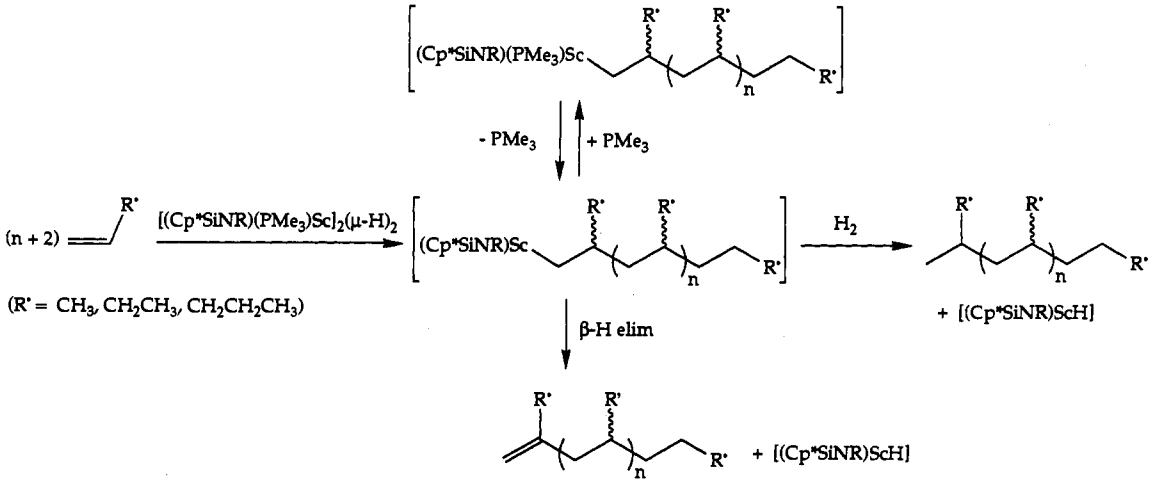

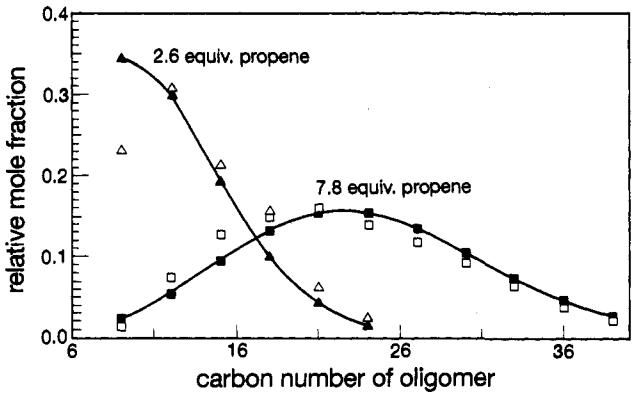

Figure 3. Experimental (open symbols) *vs* calculated Poisson (solid symbols) oligomer distributions from the reactions of **1** with 2.6 equiv (triangles) and 7.8 equiv (squares) of propene.

spectrum for all scandium alkyls, a reaction mixture of **3** with 10 equiv of propylene was allowed to react completely and subsequently treated with H_2, and the volatile products were vacuum transferred into another NMR tube. Propane (0.44 equiv per Sc) was thus collected, indicating that under these conditions 44% of the scandium propyl dimer remains, even after the 10 equiv of propylene are consumed. A likely reason for slow initiation is that the propyl-bridged dimer must cleave to more reactive monomers in order for olefin insertion to occur (*vide infra*).

Another factor contributing to broader molecular weight distribution is the slow catalyst decay for this system. The exact causes of this decay in activity have not yet been determined. Reaction of the Sc–C bond of the growing alkyl chain with the C–H (or C–D) bonds of solvent toluene is ruled out as the cause, since catalyst deactivation at similar rates also is observed in cyclohexane and methylcyclohexane. No olefinic resonances attributable to vinylidene end groups that would result from β-H elimination are apparent in the ^{1}H NMR spectrum of polypropylene produced by $[(Cp^*SiNR)Sc]_2(\mu\text{-}CH_2CH_2CH_2CH_3)_2$. Either the olefin chain ends are too dilute to be observed, or alternate forms of chain transfer (*e.g.* σ-bond metathesis with olefinic or ligand C–H bonds) are more important in this system than for the catalyst produced in the presence of phosphine, *i.e.* derived from the hydride **1**.

Kinetic Analysis of 1-Pentene Polymerization by $[(Cp^*SiNR)(PMe_3)Sc]_2(\mu\text{-}H)_2$ and $[(Cp^*SiNR)Sc]_2(\mu\text{-}CH_2CH_2CH_3)_2$. As noted above, α-olefin polymerizations using either $[(Cp^*SiNR)(PMe_3)Sc]_2(\mu\text{-}H)_2$ (**1**) or $[(Cp^*SiNR)Sc]_2(\mu\text{-}CH_2CH_2CH_3)_2$ (**3**) as catalyst precursors are relatively well behaved. By examining the kinetics of olefin polymerization using these catalyst precursors, we hoped that we could identify the true propagating scandium alkyl. The rate of disappearance of 1-pentene (^{1}H NMR) with **1** as catalyst precursor is approximately first order in 1-pentene (Figure 4). This behavior was anticipated. If the concentration of catalyst centers is constant during the polymerization and the rate of olefin insertion is independent of the size of the alkyl chain on the scandium, then simple first order disappearance of olefin should be observed. On the other hand, the apparent first-order dependence of the rate on $[\mathbf{1}]_{added}$ (Figures 4 and 5) is somewhat surprising, since added trimethylphosphine inhibits the rate of polymerization (Figure 6). The possibility that the propagating scandium alkyls in the polymerization might be dimeric, as is $[(Cp^*SiNR)Sc]_2(\mu\text{-}CH_2CH_2CH_3)_2$, further complicates interpretation of the kinetics. Thus, establishing the nature of the catalytically active scandium alkyl (with or without coordinated trimethylphosphine, monomeric or dimeric?) from analysis of the kinetics of 1-pentene polymerization, while possible in principle, is dubious.

At least two equilibria for the propagating alkyl must be considered: trimethylphosphine association (eq 6) and dimerization (eq 7).

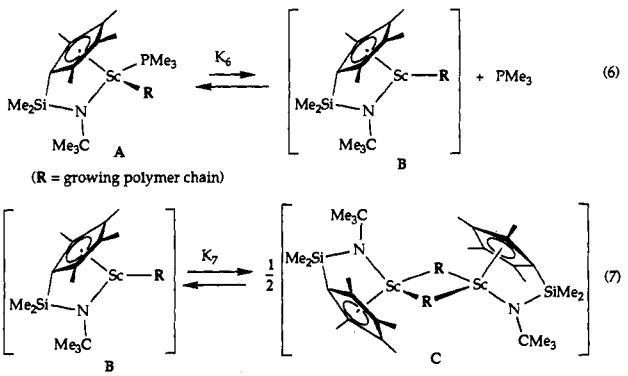

A simple situation would obtain if the propagating species were the monomeric alkyl, $[(Cp^*SiNR)Sc\text{–}\mathbf{R}]$ (**A**), that associates trimethylphosphine only weakly (K_6 large) and shows little tendency to dimerize (K_7 small). Unfortunately, the inhibition by added trimethylphosphine, even at concentrations comparable to [**1**], indicates that K_6 is, in fact, not large, and under the concentrations of **1** used for the kinetic studies trimethylphosphine-bound (**A**) and trimethylphosphine-free alkyls (**B**) are present in significant amounts. By employing the trimethylphosphine-free catalyst precursor **3**, we had hoped to address the issue of the molecularity of the trimethylphosphine-free alkyl **A**. As shown in Figure 7, the rate constant for 1-pentene polymerization (k_{obs}) does not depend linearly on $[\mathbf{3}]_{added}$. The curvature suggests that at the higher concentrations, both monomer and dimer are present

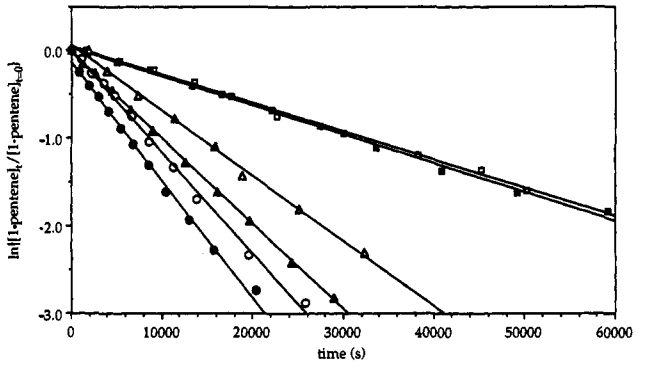

Figure 4. First-order plots for disappearance of 1-pentene for polymerization runs with [1] = 0.0095 M (□), [1] = 0.012 M (■), [1] = 0.018 M (△), [1] = 0.024 M (▲), [1] = 0.030 M (○), and [1] = 0.036 M (●).

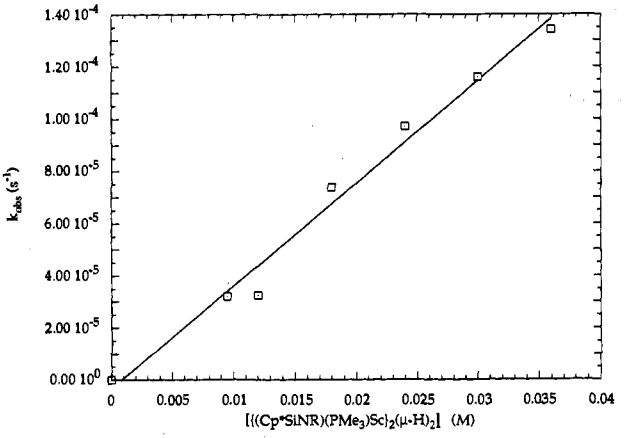

Figure 5. Dependence of the observed first-order rate constants for 1-pentene polymerization on [{(Cp*SiNR)(PMe$_3$)Sc}$_2$(μ-H)$_2$] ([1]).

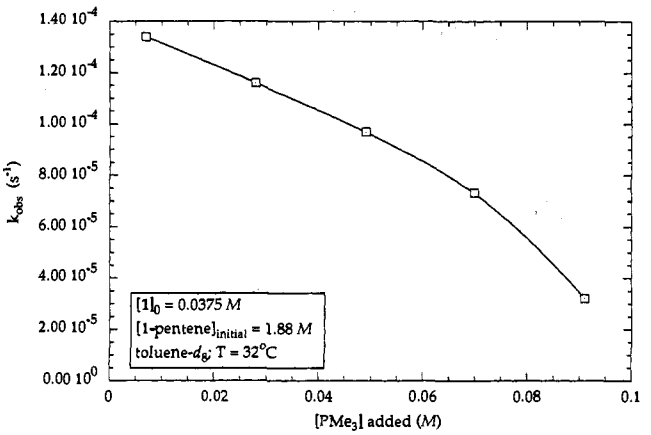

Figure 6. Dependence of the observed first-order rate constant for 1-pentene polymerization on the concentration of added trimethylphosphine with [(Cp*SiNR)(PMe$_3$)Sc]$_2$(μ-H)$_2$ as the catalyst precursor.

in comparable amounts. Thus, the kinetics of 1-pentene polymerization suggest a complex situation whereby both K_6 and K_7 are of moderate magnitude. Given the scatter in the data and the rather low stability for the catalyst, we sought other approaches to identify the active species.

Solution Dynamics of Reactive Intermediates: Measurement of Phosphine-Dissociation Equilibria and Elucidation of the Structure of the Reactive Complex in Olefin Polymerization. In order to establish the magnitudes of the equilibrium constants for eqs 6 and 7, variable-temperature NMR spectra for alkyl derivatives with β-branches, (Cp*SiNR)ScCH$_2$CHRR′ (R, R′ = alkyl) and their trimethylphosphine adducts, (Cp*SiNR)-(PMe$_3$)ScCH$_2$CHRR′, have been examined. The observed inhibition of the polymerization rate by added trimethylphosphine is consistent with two possibilities: (1) the monomeric, trimethylphosphine-free alkyl [(Cp*SiNR)Sc-**R**] reacts with α-olefin, as suggested above, or (2) the monomeric mono(trimethylphosphine) adduct [(Cp*SiNR)(PMe$_3$)Sc-**R**] reacts with α-olefin, and added PMe$_3$ generates an unreactive bis(trimethylphosphine) adduct [(Cp*SiNR)(PMe$_3$)$_2$Sc-**R**]. The second possibility may be excluded, since only (Cp*SiNR)(PMe$_3$)Sc-CH$_2$CH(CH$_3$)CH$_2$-CH$_2$CH$_3$ (**4**) and free PMe$_3$ are observed, even at −80 °C, for toluene-d_8 solutions of **4** with an equivalent of added trimethylphosphine (*vide supra*). This conclusion is fully consistent with the observations of Jordan[27] that bis(phosphine) adducts [Cp$_2$ZrR(PMe$_3$)$_2$]$^+$ are obtained only for very small R groups (R = hydride, methyl). For the zirconium compounds as for the scandium compounds described in this work, bis(phosphine) adducts of the higher alkyls are presumably destabilized by steric crowding, even in the case of the sterically more open Cp*SiNR ligand array.

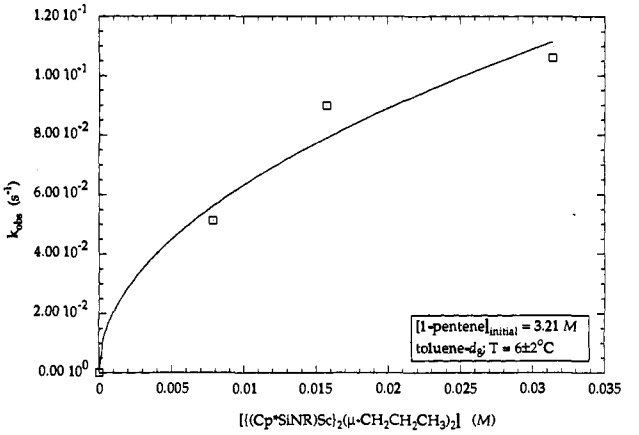

Figure 7. Dependence of the first-order rate constant for 1-pentene polymerization on [{(Cp*SiNR)Sc}$_2$(μ-CH$_2$CH$_2$CH$_3$)$_2$] ([**2**]).

In principle, it should be possible to directly observe the various species (**A**, **B**, and **C**) in equilibria 6 and 7, if their rates of interconversion can be slowed sufficiently at low temperature. The equilibrium constants could then be easily determined simply by integration, and the temperature dependence extrapolated to the temperatures employed for the polymerizations of α-olefins. Unfortunately, the ^{1}H NMR spectra of these complexes are extremely complex, especially at low temperatures, and we have not succeeded in unambiguously assigning resonances to both trimethylphosphine-bound (**A**) and -free forms (**B** and/or **C**). Accordingly, we opted to use ^{13}C NMR of appropriately labeled compounds for the purpose of measuring phosphine dissociation and dimerization equilibria. We expected that the larger chemical shift range of ^{13}C (*vis-à-vis* ^{1}H) would allow us to completely freeze out the dynamic behavior of the system and that the greatly simplified spectra resulting from the use of the specifically labeled compounds would allow us to observe and integrate resonances arising from the individual complexes.

The ^{1}H spectrum of (Cp*SiNR){P(^{13}CH$_3$)$_3$}ScCH$_2$CH-(CH$_3$)CH$_2$CH$_2$CH$_3$ (**4**-^{13}C$_3$) is complicated but the strongly ^{13}C-split pattern of the labeled phosphine is clearly visible. On the other hand, the 125-MHz ^{13}C{^{1}H} NMR spectrum at room temperature is very simple, displaying only one broadened resonance for the phosphine methyl carbons. At low temperatures free phosphine is cleanly resolved 3 ppm downfield from the scandium-bound form. As shown in Figure 8, the bound phosphine carbons appear as two $^1J_{P-C}$ doublets, providing strong evidence that two diastereomers are present in roughly equal amounts (*vide supra*).[28]

At a total scandium concentration of 0.042 M, the ^{13}C NMR resonances due to free and bound P(^{13}CH$_3$)$_3$ are cleanly resolved

(27) (a) Jordan, R. F. *Adv. Organomet. Chem.* **1991**, *32*, 325. (b) Similar chemistry is observed for THF adducts of zirconocene cations. Jordan, R. F.; Bajgur, C. S.; Willett, R.; Scott, B. *J. Am. Chem. Soc.* **1986**, *108*, 7410.

(28) Two doublets in trace amounts can be discerned between the major resonances. These cannot be identified; however, they are not observed to broaden or shift with temperature.

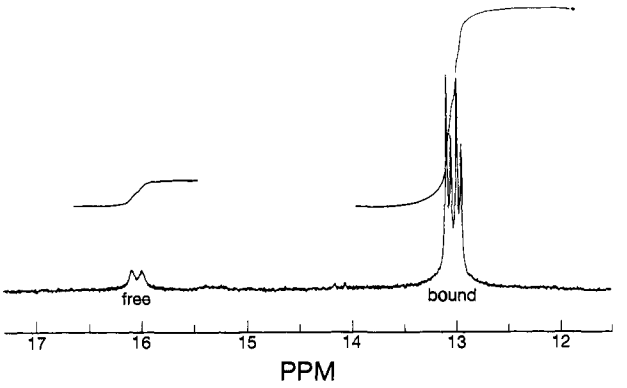

Figure 8. 125-MHz $^{13}C\{^1H\}$ NMR spectrum for (Cp*SiNR)$\{P(^{13}CH_3)_3\}ScCH_2CH(CH_3)CH_2CH_2CH_3$ (**4**-$^{13}C_3$) (0.042 M) at 200 K.

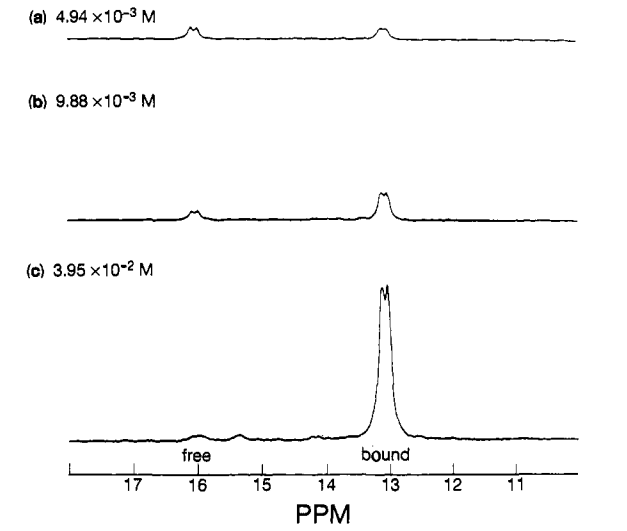

Figure 9. 125-MHz $^{13}C\{^1H\}$ NMR spectra for diluted stock toluene-d_8 solutions of (Cp*SiNR)$\{P(^{13}CH_3)_3\}ScCH_2CH(CH_3)CH_2CH_2CH_3$ (**4**-$^{13}C_3$) at 200 K.

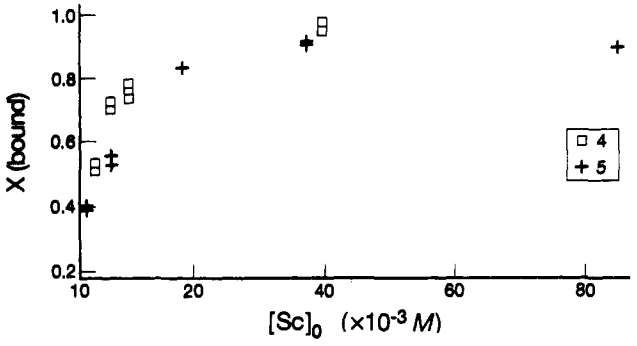

Figure 10. Equilibrium composition (mole fraction) of bound trimethylphosphine (as (Cp*SiNR)$\{P(^{13}CH_3)_3\}ScCH_2CH(CH_3)CH_2CH_2CH_3$) as a function of total scandium concentration.

between 185 and 220 K, although toward the high end of this temperature range the weaker signal of free phosphine already shows considerable broadening. The equilibrium composition of 10% free phosphine ($[PMe_3]_{free}$ = 5 mM) to 90% bound phosphine ($[PMe_3]_{bound}$ = 38 mM) does not vary significantly, so that the equilibrium constant is essentially independent of temperature over this 35 K range.

The equilibrium compositions of **4**-$^{13}C_3$ at various concentrations in toluene-d_8 solution were examined using samples prepared by sequential dilutions of a stock solution. Representative spectra appear in Figure 9. The two diastereomeric phosphine doublets are not resolved in these spectra due to a combination of lower-quality shims and application of a 5-Hz line-broadening exponential. As can be seen in Figure 10, the fractional population

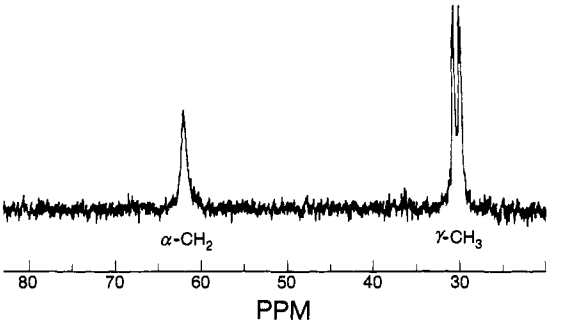

Figure 11. 125-MHz $^{13}C\{^1H\}$ NMR spectrum of (Cp*SiNR)$\{P(CH_3)_3\}Sc^{13}CH_2CH(^{13}CH_3)_2$ (**5**-$^{13}C_3$) at room temperature (*ca.* 0.08 M).

of bound trimethylphosphine shows a strong dependence on the total concentration.

Additional information concerning the structures of the solution species and their dynamics was obtained *via* incorporation of a ^{13}C label into an alkyl ligand. The isobutyl ligand for (Cp*SiNR)$\{P(CH_3)_3\}Sc^{13}CH_2CH(^{13}CH_3)_2$ (**5**-$^{13}C_3$) was chosen primarily for ease of synthesis of the labeled olefin precursor, and for its close resemblance to the 2-methylpentyl group. In addition, the diastereotopic γ-methyl groups provide useful information about the symmetry of the complexes in solution.

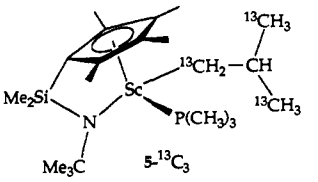

The room-temperature 125-MHz $^{13}C\{^1H\}$ NMR spectrum of **5**-$^{13}C_3$ is shown in Figure 11. Because the tetracoordinate scandium is stereogenic, the γ-methyl carbons are diastereotopic in the phosphine-bound form (**A**). They appear as a pair of doublets (the smaller coupling is due to $^2J_{C-C}$). In dilute solutions at 200 K, a *single* additional resonance in the γ-carbon region is cleanly resolved, *ca.* 7 ppm upfield of the original pair of doublets ($^2J_{C-C}$ coupling is not observed in these spectra due to the application of line broadening).[29] Figure 12 shows representative, partial low-temperature spectra over the concentration range of interest. Significantly, only two species are detected: one giving rise to a pair of inequivalent γ-methyl ^{13}C resonances attributed to **5**-$^{13}C_3$, and one giving rise to a single γ-methyl ^{13}C resonance, attributed to the trimethylphosphine-free isobutyl derivative. The abundance of the former correlates well at a given concentration with the abundance of bound $P(^{13}CH_3)_3$ in spectra for **4**-$^{13}C_3$. Significantly, we see no evidence for an additional phosphine-free isobutyl in equilibrium with **5**-$^{13}C_3$. Moreover, the observation of a single resonance for the γ-carbons of this phosphine-free species suggests that it is a monomer. As Scheme 10a shows, the monomeric complex possesses a mirror plane which makes these methyl groups strictly equivalent. The most likely structure for the dimer is analogous to that for the propyl dimer **3**, either C_i symmetric (Scheme 10b) or C_s symmetric (Scheme 10c). For both rotational conformers, 10b and 10c, the isobutyl methyl groups are diastereotopic, and should display two distinct NMR resonances.[30] Thus, the simplest explanation for the observation that only one resonance appears for the γ-methyl groups in the phosphine-free complex is that this species is monomeric.[31]

These ^{13}C NMR data for **4**-$^{13}C_3$ and **5**-$^{13}C_3$ indicate that the trimethylphosphine-free, β,β-disubstituted alkyls [(Cp*SiNR)-

(29) No corresponding α-carbon resonance is observed, presumably due to the quadrupolar broadening effect of the scandium nucleus.

(30) Even a dimer in which the cyclopentadienyl rings are *syn* to each other (C_s-**2**) should display two distinct NMR resonances.

Scheme 10

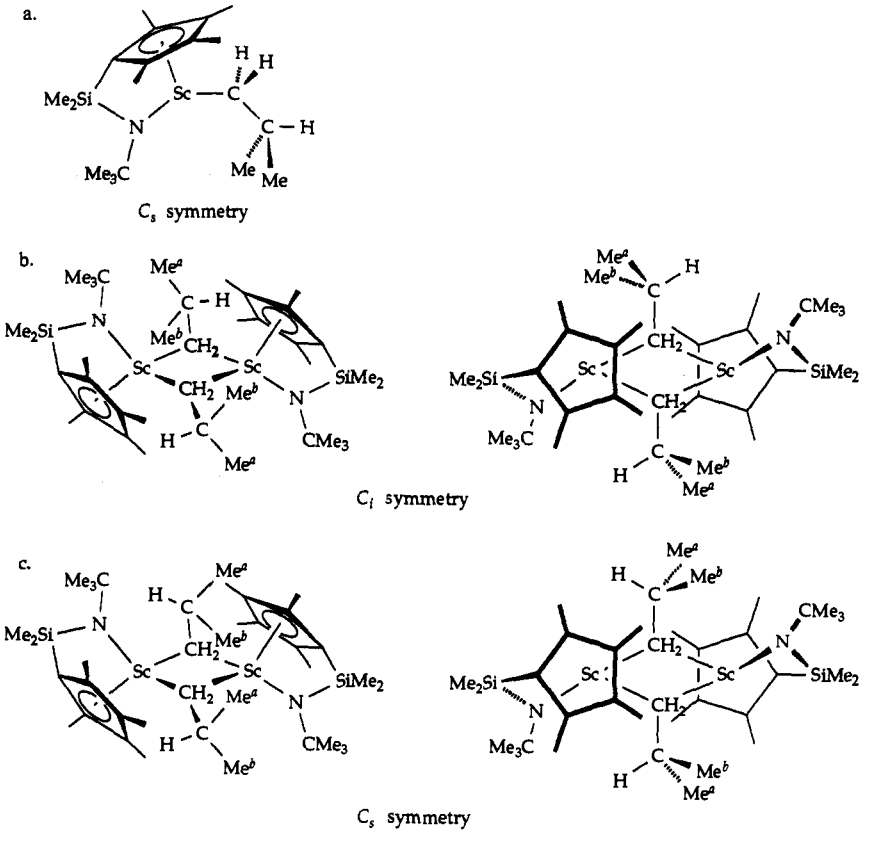

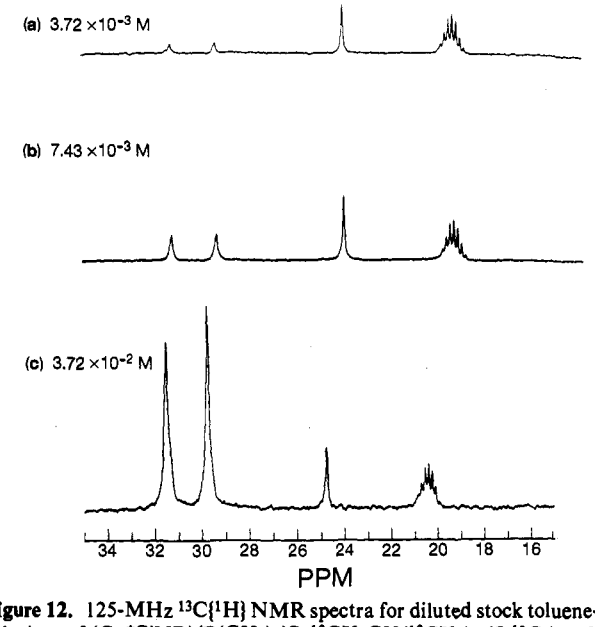

Figure 12. 125-MHz $^{13}C\{^1H\}$ NMR spectra for diluted stock toluene-d_8 solutions of (Cp*SiNR){P(CH_3)$_3$}Sc$^{13}CH_2CH(^{13}CH_3)_2$ (5-$^{13}C_3$) at 200 K.

Sc–**R**] are principally monomeric (*i.e.* K_7 for eq 7 is small). Therefore eq 8 should suffice to account quantitatively for the data in Figures 9, 10, and 12.

$$K_6 = \frac{[\mathbf{B}][PMe_3]}{[\mathbf{A}]} \qquad (8)$$

The opposite extreme with a *large* value for K_7 for eq 7 leads to the equilibrium shown in eq 9.

$$\mathbf{A} \overset{K_9}{\rightleftarrows} {}^1/_2\mathbf{C} + PMe_3 \qquad K_9 = \frac{[\mathbf{C}]^{1/2}[PMe_3]}{[\mathbf{A}]} \qquad (9)$$

If our assumption from the ^{13}C NMR spectra that the trimethylphosphine-free isobutyl complex is monomeric (and hence, all trimethylphosphine-free β,β-disubstituted alkyls are also monomeric) is correct, the data in Figures 9, 10, and 12 should be described better by equilibrium expression K_6 than by K_9. Unfortunately, this did not prove to be the case, and perhaps not surprisingly, we were faced with much the same dilemma presented by the kinetic studies. Variance in the NMR data was such that simply calculating equilibrium "constants" (K_6 or K_9) provided no clear distinction. Fortunately, in light of the arguments above, the less definitive equilibrium concentration data take on a supportive rather than a central role in analyzing this system.

The software package IGOR was used to calculate predicted concentration profiles from the equilibrium expressions K_6 and K_9. The best visual fits obtained are shown alongside the data in Figure 13. As expected, neither expression provides a completely acceptable fit.[32] However, the overall fit to the K_6 expression is significantly better than that to K_9, particularly with regard to matching the slope of the curve in the low-concentration regime with the asymptotic behavior observed in the high-concentration regime. The best estimate of K_6 that we can extract from these data is 6(3) × 10^{-4} M. This semiquantitative model of equilibrium behavior is consistent with the interpretation offered above for the NMR properties of the trimethylphosphine-free complex—namely, that for these β-branched alkyl derivatives, [(Cp*SiNR)Sc–**R**] is predominantly, if not exclusively, monomeric.[33,34]

(31) It is possible that this single resonance actually belongs to a dimer in which the diastereotopic methyl groups rapidly equilibrate. This requires that the dimeric unit break apart and reassemble after rotation about the C_β–C_γ bond. We also recognize that accidental degeneracy of formally inequivalent carbons is always a possibility. Both possibilities seem rather remote.

(32) Small experimental errors in the low-concentration regime lead to large errors in equilibrium constant, while the high-concentration regime is less susceptible to such errors.

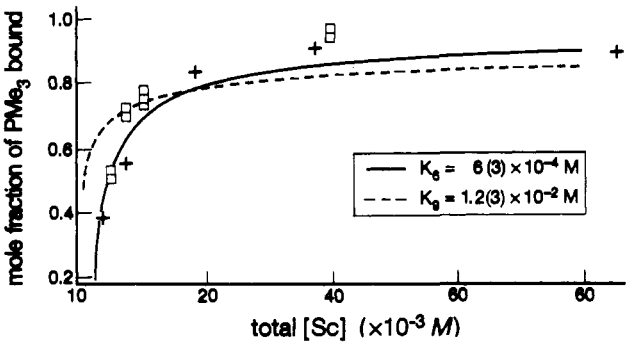

Figure 13. IGOR best fits of mole fraction of trimethylphosphine bounds *vs* [4] (□) and *vs* [5] (+) according to the expressions K_6 (solid line) and K_9 (dashed line).

The important conclusion from these equilibrium studies for the simple β-branched alkyl complexes **4** and **5** is that the active intermediates in α-olefin polymerizations with [(Cp*SiNR)Sc] alkyl or trimethylphosphine hydride derivatives as catalyst precursors are the corresponding 12-electron monomers [(Cp*SiNR)Sc**R**]. Although it is clear from the solid-state structure of the propyl derivative **3** that alkyl dimers may form, the β-branched alkyl derivatives display a reduced tendency to form dimers, likely due to the increased steric crowding.

Conclusions

The scandium hydride and alkyl complexes described above provide the first opportunity for study of α-olefin polymerization by a Ziegler–Natta catalyst in the absence of activators or co-catalysts. Polymerization is slow, at least in part due to the tendency of the propagating alkyl to associate trimethylphosphine, deactivating the reactive complex. GC/MS studies of oligomeric products indicate that the catalyst derived from the hydride complex **1** is a single component of the reaction mixture, a conclusion which is consistent with the polydispersity index of about 2 observed for poly-α-olefins. The oligomeric and polymeric products are almost completely atactic. The reduced electrophilicity of the neutral propagating alkyl, [(Cp*SiNR)Sc**R**] *vis-à-vis* the group 4 transition metal metallocene cations $[Cp_2MR]^+$, is undoubtedly a major factor in the lower activity, despite the fact that the scandium system has an additional vacant orbital and is (probably) less crowded. The higher molecular weights observed with [(Cp*SiNR)Sc**R**] *vis-à-vis* the other neutral scandium catalysts we have examined, *e.g.* $\{(\eta^5\text{-}C_5Me_4)_2SiMe_2\}$Sc–R and $\{(\eta^5\text{-}C_5H_3CMe_3)_2SiMe_2\}$Sc–R, also may be explained on the basis of steric arguments: their more crowded scandium coordination spheres disfavor propagation and favor chain transfer by β-H elimination.

The behavior reported here for [(Cp*SiNR)Sc**R**] catalysts may be compared to that observed in other Ziegler–Natta model systems. Kinetic studies of the insertion of propylene by $Cp^*_2LuCH_3\cdot(Et_2O)$ revealed a dissociative pre-equilibrium to afford the active species $[Cp^*_2LuCH_3]$. The monomeric nature of the active species was confirmed by kinetic analysis of the oligomerization of propylene by $[Cp^*_2LuCH_3]_2$.[4a] Likewise, Jordan has shown that the active species in ethylene polymerization by $[Cp_2Zr(CH_3)(L)]^+$ (L = THF, PMe_3) is the "naked alkyl", $[Cp_2Zr(CH_3)]^+$.[24] The recently prepared bulky *ansa*-yttrocene hydride $[\{(\eta^5\text{-}C_5H_2\text{-}2\text{-}SiMe_3\text{-}4\text{-}CMe_3)_2SiMe_2\}Y]_2(\mu\text{-}H)_2$ polymerizes α-olefins through intermediates which are almost certainly monomeric yttrium alkyl complexes.[35] In all of these cases, the valence electron count at the reactive metal center is 14. The scandium catalyst system reported here is unique in that, although a 14-electron species [(Cp*SiNR)(PMe_3)Sc**R**] is available and is, in fact, the predominant species in solution in the presence of trimethylphosphine at the concentrations used, it is not the reactive intermediate.

Experimental Section

General Considerations. All manipulations were performed by using glovebox and high-vacuum-line techniques as described elsewhere.[36] Solvents were dried by standard techniques and further purified by vacuum transfer from titanocene or sodium benzophenone. Argon and hydrogen were purified by passage over MnO on vermiculite and activated 4 Å molecular sieves. NMR spectra were recorded on Varian EM-390 (^{1}H, 90 MHz), JEOL FX90Q (^{1}H, 89.56 MHz; ^{13}C, 22.50 MHz; ^{31}P, 36.23 MHz), GE QE300 (^{1}H, 300 MHz; ^{13}C, 75 MHz), JEOL GX400Q (^{1}H, 399.78 MHz; ^{13}C, 100.38 MHz), and Bruker AM500 (^{1}H, 500.13 MHz; ^{13}C, 125.56 MHz) spectrometers. Infrared spectra were recorded on a Beckman 4240 spectrometer and a Perkin-Elmer 1600 series FTIR spectrometer and peak positions are reported in reciprocal centimeters. GC data were measured on a Perkin-Elmer 8410 gas chromatograph using a 10 m × 0.53 mm OV-1 macrobore column from Alltech. GC/MS data were obtained on a Hewlett Packard 5890A gas chromatograph interfaced with a Hewlett Packard 5970 series mass spectrometer, using a Hewlett Packard 12.5 m OV-1 capillary column. GPC analyses were performed on a Waters 150-C ALC/GPC with five styragel columns (10^5–100 Å porosity). Elemental analyses were performed by F. Harvey of the Caltech Analytical Laboratory. Where indicated, oxidant (V_2O_5 and WO_3) was added to the compound to facilitate burning.

Nonlinear, least-squares analysis of the kinetic data from the rate dependence of 1-pentene polymerization on added PMe_3 was performed using the program Gauss, System 2.0 (Copyright 1988, Aptech Systems Inc., Kent, WA) on an IBM PC. All other linear and nonlinear, least-squares fits were performed with the program Cricketgraph on a Macintosh computer. Spin–lattice relaxation times for all ^{13}C-labeled compounds were determined by the inversion–recovery method, using the routine INVRECX.AU on a Bruker AM500 spectrometer. ^{13}C NMR spectra were obtained using a pulse delay of at least 5 T_1. Equilibrium concentrations data were analyzed using the program Igor (copyright 1988–1990, WaveMetrics, Lake Oswego, OR 97035).

Reagents. Propene, ethylene, and HCl (Matheson) were freeze–pump–thawed at least twice prior to use. 1-Pentene (Aldrich) was dried over either titanocene or sodium sand. 1,2,4-Trichlorobenzene (Aldrich) was used as received. Cp_2Fe, used as an internal standard for NMR tube kinetics experiments, was sublimed before use. PMe_3 was either prepared as described elsewhere[37] or purchased from Aldrich. Butyllithium (1.6 M solution in hexanes) and Me_2SiCl_2 were used as obtained from Aldrich. Methyllithium and (trimethylsilyl)methyllithium (Aldrich) were used as solids obtained by drying their ether solutions. Triphenyl phosphite was dried and purified by vacuum distillation from CaH_2. $ScCl_3(THF)_3$,[38] $Li(C_5Me_4H)$,[39] and $LiCH(SiMe_3)_2$[40] were prepared as reported elsewhere.

Li_2(Cp*SiNR). $Li(C_5Me_4H)$ (23.1 g, 0.2 mol) was suspended in 250 mL of tetrahydrofuran. While the mixture was cooled to −78 °C, Me_2SiCl_2 (24.1 mL, 0.2 mol) was added via syringe. The mixture was allowed to warm to room temperature and stirred overnight. The tetrahydrofuran was removed in vacuo, leaving $(C_5Me_4)SiMe_2Cl$ as a nonvolatile, clear, colorless liquid, which was dissolved in 100 mL of petroleum ether and filtered to remove LiCl. The petroleum ether was removed in vacuo, the $(C_5Me_4)SiMe_2Cl$ was dissolved in 250 mL of THF, and $Li(Me_3CNH)$ powder was added gradually with stirring to the solution at room temperature (exothermic). The mixture was stirred for 2 hours at room temperature, and the THF was removed in vacuo and replaced with 100

(33) Similar equilibrium measurements for solutions of $[(Cp^*SiNR)Sc]_2(\mu\text{-}CH_2CH_2CH_3)_2$ (**3**) with $P(^{13}CH_3)_3$ produced data that could be fit fairly well to the "coupled" equilibrium situation (eqs 6 and 7) using IGOR. The best visual fit gives $K_6 = 6 \times 10^{-4}$ M and $K_7 = 8$ M$^{-1/2}$.

(34) As expected, an improved fit can be obtained by assuming an intermediate value for K_7 (*i.e.* rather than assuming essentially none of [(Cp*SiNR)Sc-**R**] dimerizes, allowing for a small amount to form dimer **C**), since this provides an additional parameter for the fit. Given the scatter in our data, however, we see no justification for pursuing this approach to evaluate K_7.

(35) Coughlin, E. B.; Bercaw, J. E. *J. Am. Chem. Soc.* **1992**, *114*, 7606.

(36) Burger, B. J.; Bercaw, J. E. In *Experimental Organometallic Chemistry*; Wayda, A. L., Darensbourg, M. Y., Eds.; ACS Symp. Ser. No. 357; American Chemical Society: Washington, DC, 1987; pp 79–98.

(37) (a) Wolfsberger, W.; Schmidbaur, H. *Synth. React. Inorg. Met.-Org. Chem.* **1974**, *4*, 149–156. (b) Sharp, P. R. *Organometallics* **1984**, *3*, 1217–1223. (c) Gibson, V. C.; Graimann, C. E.; Hare, P. M.; Green, M. L. H.; Bandy, J. A.; Grebnik, P. K.; Prout, K. *J. Chem. Soc., Dalton Trans.* **1985**, 2025–2035.

(38) Manzer, L. E. *Inorg. Syn.* **1982**, *21*, 135.

(39) Bunel, E. Ph.D. Thesis, California Institute of Technology, 1988.

(40) (a) Cowley, A. H.; Kemp, R. A. *Synth. React. Inorg. Met.-Org. Chem.* **1981**, *11* (6), 591. (b) Davidson, P. J.; Harris, D. H.; Lappert, M. F. *J. Chem. Soc., Dalton Trans.* **1976**, 2268.

mL of petroleum ether. LiCl was filtered off and the petroleum ether was removed in vacuo to afford H_2Cp^*SiNR as an orange oil. [Alternatively, to a cold (−78 °C) solution of $(C_5Me_4)SiMe_2Cl$ (92 mmol) in petroleum ether (~250 mL), *tert*-butylamine (19.4 mL, 13.5 g, 2.00 equiv) is added by syringe. The reaction mixture is warmed to room temperature with stirring. The reaction mixture is stirred overnight and *tert*-butylammonium chloride is removed by filtration. Removal of solvent *in vacuo* leaves the crude product as a yellow oil, which is vacuum distilled. The product distills as the second fraction (bp ~70 °C at 10^{-3} Torr), a pale, yellow-green liquid (16.9 g, 71.0 mmol, 76.4%).]

H_2Cp^*SiNR was dissolved in 100 mL of diethyl ether and cooled to −78 °C. *n*-Butyllithium (1.6 M in hexanes, 250 mL, 0.4 mol) was added via syringe and the reaction was allowed to warm to room temperature. After the reaction was stirred overnight the precipitated $Li_2(Cp^*SiNR)$ was collected by filtration as a tan powder (45.2 g, 80.7% yield).

(Cp*SiNR)ScCl. $Li_2(Cp^*SiNR)$ (16.8 g, 64 mmol) and $ScCl_3(THF)_3$ (23.5 g, 64 mmol) were combined with 250 mL of toluene and stirred overnight at room temperature. The resulting solution was filtered and the toluene was removed in vacuo, leaving an orange oil. Addition of petroleum ether (ca. 100 mL) precipitated a white solid. Three crops were obtained. The solid was loaded into a flask and heated at 100 °C under dynamic vacuum overnight to remove the THF. The product was then extracted away from the LiCl with hot toluene. The toluene was removed in vacuo, and petroleum ether was added to the resulting orange oil to precipitate (Cp*SiNR)ScCl as a white powder (10.4 g, 51% yield). Elemental Anal. Found (Calcd): C, 54.14 (54.45); H, 7.90 (8.22); N, 4.23 (3.93). IR (Nujol): 2733, 2686, 1465, 1372, 1349, 1320, 1244, 1198, 1122, 1076, 1046, 1029, 849, 826, 802, 756, 692, 552, 500.

(Cp*SiNR)ScCH{Si(CH$_3$)$_3$}$_2$. (Cp*SiNR)ScCl (3.0 g, 9.1 mmol) and $LiCH(TMS)_2 \cdot {}^1/_2Et_2O$ (1.85 g, 9.1 mmol) were combined in 150 mL of toluene and stirred at 80 °C for approximately 1 h and then overnight at room temperature. Toluene was removed in vacuo and the residue was redissolved in petroleum ether and filtered to remove the LiCl. The product was then precipitated at −78 °C as a white microcrystalline solid (3.12 g, yield 76%). Elemental Anal. Found (Calcd): C, 58.0 (58.1); H, 10.0 (10.2); N 3.0 (3.1). IR (Nujol): 2756, 2663, 1453, 1372, 1360, 1302, 1232, 1186, 1023, 860, 837, 814, 790, 767, 756, 721, 663, 599, 581, 535, 488.

[(Cp*SiNR)(PMe$_3$)Sc]$_2$(μ-H)$_2$ (1). (Cp*SiNR)ScCH{Si(CH$_3$)$_3$}$_2$ (1.04 g, 2.3 mmol) was partially dissolved in 30 mL of petroleum ether in a thick-walled glass vessel and 0.23 mL of PMe_3 (2.3 mmol) was added by vacuum transfer. H_2 (4 atm) was added to the vessel and the reaction mixture was stirred at room temperature. After 15 min the solid was completely dissolved, leaving a yellowish solution. Upon continued stirring, a white precipitate formed. The reaction was stirred overnight and **1** was collected by filtration as a white powdery precipitate (0.71 g, 83% yield). Elemental Anal. Found (Calcd): C, 58.6 (58.0); H, 9.8 (10.0); N, 3.2 (3.8). IR (Nujol): 2704, 2670, 1459, 1375, 1352, 1335, 1328, 1279, 1240, 1299, 1226, 1200, 1152, 1130, 1031, 1014, 950, 936, 837, 814, 795, 738, 671, 662, 623.

[(Cp*SiNR)(PMe$_3$)Sc]$_2$(μ,η^2,η^2-C$_2$H$_4$) (2). Compound **1** (0.308 g, 0.414 mmol) was dissolved in 10 mL of toluene in a thick-walled glass vessel. Two equivalents of ethylene (148 Torr, 104.3 mL), 1 equiv per scandium, were condensed into the reaction mixture at −196 °C. The reaction was thawed at −80 °C and then stirred at 0 °C for 2 h. The resulting yellow solution was warmed to room temperature and then transferred to a flask attached to a swivel frit assembly in a glovebox. The solution was concentrated to ca. 5 mL and cooled to −80 °C for 3 h to afford orange-yellow crystals of $[(Cp^*SiNR)(PMe_3)Sc]_2(\mu,\eta^2,\eta^2\text{-}C_2H_4)$ (0.170 g, 53%). Elemental Anal. (oxidant added; two sets of data reported) Found: C, 61.53, 63.64; H, 9.31, 9.71; N, 3.07, 3.19. Calcd.: C, 62.8; H, 9.8; N, 3.25.

[(Cp*SiNR)Sc]$_2$(μ-CH$_2$CH$_2$CH$_3$)$_2$ (3). Compound **1** (0.531 g, 0.787 mmol) was dissolved in 20 mL of toluene in a thick-walled glass vessel. Two equivalents of propene (256 Torr, 104.3 mL), 1 equiv per scandium, were condensed into the reaction mixture at −196 °C. After the mixture was warmed slowly to 25 °C, the reaction was stirred for 15 min. The solution was then transferred to a flask attached to a swivel frit assembly in a glovebox. The solvent was removed under reduced pressure and the resulting white solid was suspended in 5 mL of petroleum ether, filtered, and washed once with another portion of petroleum ether to afford a white powder (0.156 g, 32%). Elemental Anal. (oxidant added, two sets of data reported) Found: C, 64.87, 63.13; H, 10.07, 9.76; N, 4.56, 4.40. Calcd.: C, 64.0; H, 10.2; N, 4.1. IR (Nujol): 2720, 1455, 1375, 1350, 1320, 1240, 1190, 1120, 1035, 1010, 840, 815, 790, 760, 740, 470.

[(Cp*SiNR)Sc]$_2$(μ-CH$_2$CH$_2$CH$_2$CH$_3$)$_2$. The same procedure was used as is described above for **6**, except that 1-butene (192 Torr, 104.3 mL) was added to a toluene solution of **1** (0.4 g, 0.54 mmol). The resulting white solid was redissolved in 10 mL of toluene and the volatiles were then removed in vacuo. This cycle was repeated three times to ensure complete removal of PMe_3 from the product. Yield 0.173 g, 37.6%. Elemental Anal. Found (Calcd): C, 64.91 (64.9); H, 10.09 (10.3), N 4.16 (4.0). IR (Nujol): 2720, 1455, 1378, 1355, 1320, 1243, 1226, 1196, 1126, 1096, 1079, 1038, 1014, 944, 838, 814, 797, 762, 744, 668, 532, 497, 480.

(Cp*SiNR)(PMe$_3$)ScCH$_2$CH(CH$_3$)CH$_2$CH$_2$CH$_3$ (4). 2-Methyl-1-pentene (2.2 equiv, 251 Torr, 104.3 mL) was condensed into a solution of **1** (0.50 g, 1.3 mmol) in 15 mL of toluene at −196 °C. The reaction mixture was warmed to room temperature and stirred for 2 days. Removal of the solvent under reduced pressure afforded a golden brown oil which was dissolved in 2–3 mL of pentane and cooled to −78 °C to afford white crystals (0.298 g, 50.3%). Elemental Anal. Found (Calcd): C, 62.7 (63.3); H, 10.4 (10.8); N, 2.8 (3.1). IR (Nujol): 2708, 1461, 1372, 1355, 1308, 1284, 1237, 1196, 1138, 1126, 1032, 1014, 961, 950, 891, 838, 814, 785, 756, 738, 662, 532, 520, 497, 479. **4**-$^{13}C_3$ was prepared in the same way, except that $P(^{13}CH_3)_3$ (*vide infra*) was used in the preparation of the hydride precursor.

(Cp*SiNR)(PMe$_3$)ScCH(C$_6$H$_5$)CH$_2$CH$_2$CH$_2$C$_6$H$_5$. To a solution of compound **1** (0.20 g, 0.54 mmol) in 15 mL of toluene was added 125 μL (1.1 mmol) of styrene by syringe in a glovebox. The reaction was stirred at room temperature for 1 h. The volatiles were removed from the resulting orange-yellow solution under reduced pressure leaving a yellow solid which was redissolved in petroleum ether. Cooling the solution to −78 °C afforded a bright, canary yellow, microcrystalline solid (2 crops: 0.253 g, 81%). Elemental Anal. Found (Calcd): C, 70.22 (70.4); H, 8.96 (9.2); N 2.2 (2.4). IR (Nujol): 2750, 2700, 1584, 1455, 1376, 1352, 1308, 1258, 1199, 1093, 1026, 838, 811, 800, 747, 697, 597, 565, 535, 523, 500, 479.

(^{13}C$_3$)Trimethylphosphine. The procedure described here represents a modification of published procedures, adapted to a sufficiently small scale to allow for the economical use of $^{13}CH_3I$.[37] Magnesium turnings (0.206 g) were slurried in anhydrous dibutyl ether (50 mL, Aldrich) in a 250-mL three-necked flask, equipped with a reflux condensor, N_2 flush inlet, and stir bar. With the flask in a bath of room-temperature water, iodomethane-^{13}C (20 g, 0.140 mmol) was added dropwise. The Grignard solution was then cooled to 0 °C. An addition funnel was charged with dry triphenyl phosphite (11 g, 0.035 mmol) and dibutyl ether (20 mL). This solution was added dropwise to the ice-cooled Grignard mixture. When addition was complete, a distillation head was attached to the top of the reflux condensor and the ice bath was replaced with a heating mantle. The coils of the reflux condensor were filled with water, although water was not circulated through the coils continuously. The reaction mixture was then heated until dibutyl ether refluxed vigorously. The product phosphine was slowly liberated from the mixture and distilled (2.89 g, crude). (During practice runs with non-labeled methyl iodide, several different distillation setups were tried. Use of a filled, non-circulating reflux condensor was found to facilitate the simultaneous maintenance of dibutyl ether reflux while allowing the phosphine to distill.) The crude product contained a small amount of dibutyl ether and was distilled once more before use (1.88 g, 71% overall yield).

(1,3,3-^{13}C$_3$)-2-Methylpropene. To a toluene (20 mL) solution of triphenylphosphine (3.22 g, 12.3 mmol) was added $^{13}CH_3I$ (0.80 mL, 1.8 g, 12.6 mmol). The mixture was stirred overnight. The precipitate was collected, dried in vacuo, and removed to a drybox, where it was slurried in anhydrous diglyme (80 mL, Aldrich). Mineral oil-free KH (560 mg, 14 mmol) was added to the mixture. Under argon on a Schlenk line, the reaction mixture was heated to 100 °C, stirred overnight, and cooled to room temperature. Against an argon counterflow, (1,3-$^{13}C_2$)-acetone (0.90 mL, 12.3 mmol) was added via syringe. Upon addition of acetone, the reaction mixture became noticeably warm. When it had cooled, it was degassed through a liquid nitrogen-cooled trap. The condensed volatiles were distilled twice on a vacuum line from −60 °C (acetonitrile slurry) traps. The product was stored over lithium aluminum hydride in a glass bomb (521 mg, 70%).

(Cp*SiNR)Sc(^{13}CH$_2$CH(^{13}CH$_3$)$_2$)·P(CH$_3$)$_3$ (5-^{13}C$_3$). **1** (360 mg, 0.969 mmol) was dissolved in toluene (5 mL) in a 10-mL round-bottomed flask on a thin-bodied swivel frit. (1,3,3-$^{13}C_3$)-2-methylpropene was added via condensation from a calibrated volume (770 Torr in 33.5 mL, 1.39 mmol) and the reaction mixture was stirred at room temperature for 1 h. Volatiles were removed and the product was isolated from petroleum ether solution. The isolated product was found to consist of ca. 20% $[(Cp^*SiNR)ScH(PMe_3)]_2$, so all solids were returned to the reaction vessel, redissolved in toluene (5 mL), treated with a additional portion of (1,3,3-$^{13}C_3$)-2-methylpropene (134 Torr in 33.5 mL, 0.243 mmol) and

allowed to stir overnight at room temperature. Volatiles were removed to obtain a yellow oil which slowly deposited a crystalline solid. Recrystallization from petroleum ether afforded the product as a cream-colored microcrystalline solid (135.5 mg, 0.3147 mmol, 32.5%). Satisfactory elemental analyses of this compound were not obtained, due to incomplete combustion.

Toepler Experiment To Determine the Amount of Ethane Produced in the Formation of 2. Compound **1** (45.5 mg, 0.0612 mmol) was dissolved in 2.5 mL of toluene in a small (5 mL) glass vessel equipped with a Kontes valve. Ethylene (0.12 mmol, 57 Torr, 40.1 mL) was admitted to the frozen reaction mixture at −196 °C. The reaction mixture was thawed at −80 °C and stirred at 0 °C for 1 h and then at 25 °C for 15 min. The volatiles from the reaction, including solvent, were vacuum transferred to a larger-volume (ca. 25 mL) thick-walled vessel and were kept at −8 °C during the Toepler measurement. The amount of gas measured (43 ± 1 Torr, 25.2 mL; 0.58 ± 0.02 mmol) corresponds to 95.5% of the theoretical amount of ethane expected. IR analysis of the gas confirmed its identity as ethane.

Sample Polymer Syntheses. (a) Poly-1-butene Synthesis by 1. To a solution of compound **1** (0.03 g, 0.04 mmol) in 5 mL of toluene in a thick-walled glass vessel was added ca. 1600 equiv of 1-butene (790 Torr, 1.5 L) at −196 °C. After the solution was stirred for 7 days at room temperature, the reaction was quenched by the addition of 0.3 mL of methanol against an argon counterflow. The scandium was removed from the polymer product by extraction of the toluene solution with dilute HCl. The toluene phase was dried over $MgSO_4$, and the toluene was then removed under reduced pressure to afford 2.5 g of polymer with a number average molecular weight of 4000 and a PDI of 1.7 (GPC *vs* polystyrene).

(b) Poly-1-pentene Synthesis by 1. Compound **1** (0.031 g, 0.042 mmol) was dissolved in 10.8 mL of 1-pentene and the reaction was stirred at room temperature for 19 h. The reaction was quenched with 2 mL of methanol, and the excess pentene was removed under vacuum. The residue was dissolved in ethyl ether and extracted with 6 M HCl followed by saturated, aqueous $NaHCO_3$ and then water. The ether phase was dried over $MgSO_4$, and the ether was removed under reduced pressure to afford 5 g of polymer with a number-average molecular weight of 2900 and a PDI of 2.08 (GPC *vs* polystyrene). The reaction was carried out in a similar fashion at 0 °C in a constant temperature bath (37 mg of **4**, 10.2 mL of pentene) to afford after ca. 25 h 0.044 g of polypentene (M_n = 7000, PDI = 1.7).

(c) Polypropene Synthesis by 3. Approximately 0.016 mol of propene (760 Torr, 0.4 L) was stirred over titanocene at −80 °C and then condensed onto a solution of **3** (21.5 mg, 0.032 mmol) in 2.5 mL of toluene at −196 °C. The reaction was stirred for approximately 5 h while submerged in a constant temperature bath set at 24 °C. The reaction was quenched at this temperature by the addition of ca. 1 mL of MeOH against an argon counterflow. The resulting toluene solution was extracted with dilute HCl and dried over $MgSO_4$, and the toluene was removed under reduced pressure to afford 0.5 g of polymer. M_n = 5206, PDI = 2.75 (GPC *vs* polystyrene). The reaction was carried out in a similar fashion at a constant temperature of −9 °C to afford 0.6 g of polymer (M_n = 16500, PDI = 1.7).

Oligomer Molecular Weight Distributions. In a standard oligomerization run, propene (3–8 equiv) was measured into a calibrated gas volume and condensed at −196 °C into a small reaction vessel containing a 0.5-mL solution of **3** (ca. 0.1 M) in toluene-d_8. The reaction mixture was stirred at room temperature for 1–2 h. The volatiles were then vacuum-transferred into an NMR tube at −196 °C along with a measured amount of hexamethyldisiloxane. The amount of unreacted propene was determined by integrating it relative to the hexamethyldisiloxane standard at −80 °C by ^{1}H NMR spectroscopy. The reaction residue containing the propene insertion products was redissolved in ca. 1 mL of benzene and stirred under 4 atm of H_2 at room temperature overnight. The resulting mixture was exposed to air and immediately passed through a plug of silica gel to remove all scandium byproducts, and the solution of saturated oligomers was analyzed by GC and GC/MS. Because of the unavailability of authentic hydrocarbon standards, GC/MS was used to verify the identity of the oligomers. The response factors of the oligomers, using flame-ionization detection, were assumed to be linearly related to their carbon number and were scaled accordingly.

Sample Kinetic Procedure: Kinetic Analysis of 1-Pentene Polymerization by 1. Rate Dependence on Scandium Concentration. In a glovebox, a stock solution was prepared by dissolving 100.3 mg of **4** and 126.8 mg of Cp_2Fe in 3 mL of toluene-d_8. Serial dilutions of the stock solution were prepared in five different NMR tubes by adding the appropriate amount of toluene-d_8 to 0.2-, 0.3-, 0.4-, 0.5-, and 0.6-mL aliquots of the stock solution to bring the final volume of each sample to 0.6 mL. Each NMR tube had a 14/20 ground-glass joint, which could be attached to a needle valve. To add 1-pentene to each sample, the NMR tube/needle valve assembly was attached to a 104.3-mL gas volume on the vacuum line. The sample was frozen at −196 °C, the NMR tube was evacuated, and 240 Torr of 1-pentene were admitted to the gas bulb and then condensed into the NMR tube. The pentene was estimated to contribute an additional 0.15 mL to the volume of the sample in calculating concentrations of catalyst and olefin. The tube was then sealed with a torch and stored at −196 °C prior to the experiment.

Each NMR tube sample was fully submerged in a 32 °C oil bath and removed at regular intervals to monitor the change in 1-pentene concentration relative to the internal ferrocene standard on an EM390 ^{1}H NMR spectrometer, probe temperature 32 °C. Spectra were generally recorded over the duration of 3–4 half-lives for each sample.

Generation of Propene Trimers by 1 for GC Analysis. Three equivalents of propene (23 Torr, 132.6) were condensed from a gas bulb into a solution containing 20.0 mg (0.054 mmol) of **1** in 1–2 mL of benzene in a thick-walled vessel cooled to −196 °C.

Sample Equilibrium Concentrations Procedure: Preparation of (Cp*SiNR)Sc[$CH_2CH(CH_3)CH_2CH_2CH_3$][P($^{13}CH_3$)$_3$] Samples for NMR Analysis. A stock solution of (Cp*SiNR)Sc[$CH_2CH(CH_3)CH_2CH_2CH_3$][P($^{13}CH_3$)$_3$] (18.1 mg, 0.0395 mmol) was prepared in toluene-d_8 (1.00 mL, 0.0395 M). Samples were prepared adding sample and diluent (volumes were measured by 100- or 1000-μL Hamilton syringe, as appropriate) directly to sealable 5-mm NMR tubes. These were frozen, degassed on the vacuum line, and sealed for analysis.

X-ray Crystal Structure Determination of [(Cp*SiNR)(PMe$_3$)Sc]$_2$(μ,η^2,η^2-C_2H_4). Orange-yellow crystals were grown from a toluene solution of [(Cp*SiNR)(PMe$_3$)Sc]$_2$(μ,η^2,η^2-C_2H_4) cooled at −60 °C. A roughly cubic crystal was cut with a razor blade from a large hexagonal prism and held inside a 0.5-mm capillary with some hydrocarbon grease. The crystal was centered on the diffractometer and 25 reflections with $18° < 2\theta < 21°$ were found and centered. Preliminary cell dimensions and the orientation matrix were obtained from their setting angles; final cell dimensions were calculated from the setting angles of 25 different reflections with $32° < 2\theta < 40°$. The compound crystallizes in the monoclinic system in space group $C2/c$ (No. 15), with a = 23.706(5) Å, b = 11.342(2) Å, c = 21.141(3) Å, β = 111.57(1)°, and volume = 5286.2(17) Å^3; Z = 4. Two equivalent sets of data were collected and merged to give the final data set; the R-factor for merging was 0.055. The data were corrected for a slight (0.2%) decay, but no absorption correction was applied because μr_{max} was small and the grease obscured the edges of the crystal. The structure was solved by MULTAN and refined by full-matrix least squares. A toluene solvent molecule was found early on, disordered about a center of symmetry, and its carbon atoms were included as constant contributions to the structure factors, but their parameters were not refined. Hydrogen atoms attached to the methyl groups were positioned at idealized positions based on difference maps calculated in their planes; of the 12 methyl groups, 11 showed clearly 3 hydrogen atoms in reasonable positions. The last, C8, had 6 possible locations, so two sets of half-hydrogens were introduced there. All these were fixed in position, with arbitrary (7.0 Å^2) thermal parameters. The two hydrogen atoms on the bridging ethylene molecule were located in a difference map and their positional and thermal parameters were refined. The refinement converged quickly; the final R-index for reflections with $F_o^2 > 3\sigma(F_o^2)$ is 0.069. The final goodness of fit, 3.84, is rather high; this probably reflects problems in modelling the disordered toluene solvate, because the three highest peaks, and 6 of the top 9, in the final difference map are in this region (0.7, 0.7, and 0.5 e Å^{-3}); the next highest peaks are less than 0.5 e Å^{-3}, two near the Cp* ring and one near the *tert*-butyl group on nitrogen. All other peaks are less than 0.4 e Å^{-3}. There are 4 negative peaks in the difference map with magnitude greater than 0.4 e Å^3; all are in the solvent region, the largest, −0.8 e Å^{-3}, near C21. Unfortunately, the peaks and holes do not suggest a different model for this region.

X-ray Crystal Structure Determination of [(Cp*SiNR)Sc]$_2$(μ-$CH_2CH_2CH_3$)$_2$ (3). Crystals of **3** were grown from a benzene solution cooled to ca. 5 °C and mounted in glass capillary tubes. Most were twinned, but one was found whose rotation photograph was acceptable. The capillary was large and the crystal was obscured by grease inside it, so we could not determine its size or shape precisely. The crystal was centered on the diffractometer and unit cell dimensions plus an orientation matrix were calculated from the setting angles of 25 reflections with $2\theta \approx 20°$. Final unit cell dimensions were obtained later from 24 reflections with $31° < 2\theta < 35°$. The crystal was monoclinic, space group $P2_1/n$ (No. 14), with a = 9.429(2) Å, b = 21.937(5) Å, c = 9.826(2) Å, β = 99.39(2)°, and volume = 2005.2(7) Å^3; Z = 2. Two equivalent sets of data were collected; there was no decay in the crystal as measured by the

three check reflections that we monitored during data collection. The data were corrected for background, Lorentz and polarization factors were applied, and the data were merged to give one set that was put on an approximately absolute scale by Wilson's method. The locations of the scandium and silicon atoms were found by MULTAN and the remainder of the atoms were located in a subsequent Fourier map. Full-matrix least squares, first with isotropic and then with anisotropic thermal parameters for the non-hydrogen atoms, converged with an R-index of about 15%. A disorder in the methyl atoms of the *tert*-butyl group was noted and an alternate orientation of those three carbon atoms was added, with the population fixed at 20% of the total. Hydrogen atoms were added, either at calculated positions or based on difference maps calculated in their planes, on all carbon atoms except C20, the bridging atom, and the minor component of the *tert*-butyl group. The hydrogen atoms were given isotropic thermal parameters 20% greater than the equivalent isotropic thermal parameter of the bonded carbon atom; neither their positions, nor their thermal parameters, nor the parameters of the *tert*-butyl component (whose isotropic thermal parameters were fixed at the average of the equivalent isotropic thermal parameters of the three major carbon atoms) were refined. Further refinement converged with an R-index of about 9% and a goodness of fit of 2.65. Most peaks in the difference map (maximum height ±0.62 e Å^{-3}) were in the region of the bridging *n*-propyl group, but a chemically reasonable model for an alternate bridging group could not be found. The two hydrogen atoms on the bridging carbon atom C20 were located and included as fixed contributions along with the rest of the hydrogen atoms (repositioned) and the minor component of the *tert*-butyl group, and the refinement was completed. The final R-index is 0.0854; for those reflections with $F_o^2 > 3\sigma(F_o^2)$, $R = 0.0579$. The goodness of fit is 2.36. The final difference map had excursions of +0.48 and −0.45 e Å^{-3}. The largest peak is about equidistant from the three atoms of the bridging propyl group, still suggesting that the model is inadequate, but the small size of the residual peaks indicates that whatever disorder exists in this region is minor.

Calculations were done with programs of the CRYM Crystallographic Computing System and ORTEP. Scattering factors and corrections for anomalous scattering were taken from a standard reference.[41]

Acknowledgment. This work has been supported by USDOE Office of Basic Energy Sciences (Grant No. DE-FG03-85ER113431) and by Exxon Chemicals America.

Supplementary Material Available: Details of the structure determinations, including listings of final atomic coordinates, thermal parameters, and bond distances and angles (8 pages); listing of observed and calculated structure factors (24 pages). This material is contained in many libraries on microfiche, immediately follows this article in the microfilm version of the journal, and can be ordered from the ACS; see any current masthead page for ordering information.

(41) *International Tables for X-ray Crystallography*; Kynoch Press: Birmingham, 1974; Vol. IV, pp 71 and 149.